An-Najah National University

Faculty of Graduate Studies

Indoor Radon Concentration Measurements in Dwellings in Tammoun Town, Palestine

By

Mohammad Mahmoud Omar Bsharat

Supervisor

Prof. Ghassan Saffarini

This Thesis is Submitted in Partial Fulfillment of the Requirements for the Degree of Master of Science in Physics, Faculty of Graduate Studies, An-Najah National University, Nablus, Palestine.

2020

Indoor Radon Concentration Measurements in Dwellings in Tammoun Town, Palestine

By

Mohammad Mahmoud Omar Bsharat

This thesis was defended successfully on 24/6/2020 and approved by:

Defense committee Members	**Signature**
- Prof. Ghassan Saffarini / Supervisor	.....
- Dr. Hussien Shanak / External Examiner	.....
- Dr. Musa El-hasan / Internal Examiner	.....

Dedication

To my beloved parents who partied nights until I got to this place…

To my brothers and sisters …

To my dear wife (Maymona) for her encouragement patience, and support…

To my beloved children (Sohaib & Khaled & Hussam) …

To all my friends, family, and those who are looking forward for more knowledge… with respect and love…

Acknowledgment

First and foremost, I would like to thank God Almighty for giving me the strength, knowledge, ability and opportunity to undertake this research study and to persevere and complete it satisfactorily. Without his blessings, this achievement would not have been possible.

I would like also to sincerely thank my supervisor Prof. Ghassan Saffarini for his guidance, understanding, patience and most importantly, he has provided positive encouragement and a warm spirit to finish this thesis. It has been a great pleasure and honor to have him as my supervisor.

Thanks and appreciations are extended to the people who provided me their support all long my master study. Also people who opened the doors of their homes to me, in order to put radon detectors inside them to complete this study.

Finally, I would like also to express my sincere thanks to An-Najah National University providing all the required resources and support to finish my thesis, especially Physics, Chemistry, and Biotechnology Departments' Laboratory staff…

الإقرار

أنا الموقع أدناه مقدم الرسالة التي تحمل عنوان

Indoor Radon Concentration Measurements in Dwellings in Tammoun Town, Palestine

أقر بأن ما اشتملت عليه هذه الرسالة، إنما هي نتاج جهدي الخاص، باستثناء ما تمت الإشارة إليه حيثما ورد، وأن هذه الرسالة ككل، أو أي جزء منها لم يقدم لنيل أي درجة علمية، أو بحث علمي أو بحثي لدى أي مؤسسة تعليمية أو بحثية أخرى.

Declaration

The work provided in this Thesis, unless otherwise referenced, is the researcher's own work, and has not been submitted elsewhere for any other degree or qualification.

Student's name: **اسم الطالب:**

Signature: **التوقيع:**

Date: **التاريخ:**

Table of Contents

List of Tables

List of Figures

List of Abbreviations

AEDE:	Absorption effective dose equivalent
Bq/m^3:	Becquerel per cubic meter
EPA	Environment Protection Agency
ICRP:	International Commission on Radiological Protection
MeV:	Million electron Volts
mSv/y:	MilliSievert per year
NaOH:	Sodium Hydroxide
PAEC:	Potential Alpha Energy Concentration
SD:	Standard Deviation
SE:	Standard Error
SSNTDs:	Solid-State Nuclear Track Detectors
WHO:	World Health Organization
WL:	Working Level
WLM:	Working Level per Month

Indoor Radon Concentration Measurements in Dwellings in Tammoun Town, Palestine

By
Mohammad Mahmoud Omar Bsharat
Supervised by
Prof. Ghassan Saffarini

Abstract

Radon is the leading cause of lung cancer after smoking, so many studies are conducted to determine the concentration of radon inside the homes in order to reduce its harm to people.

The objective of this study is to find the level of radon concentration in the houses of Tammoun town using passive radon measurement technique with alpha track detectors CR-39.

During the three-month period, the dosimeters were distributed to different rooms located in several areas at different floors. The detectors were then collected for chemical etching with 6.25 N NaOH solution at 75 ° C for 6 hours.

The radon concentration in Tammoun town dwellings varied from 16.07 to 56.60 with average of 28.98 ± 1.22 Bq/m^3. For the annual effective dose for the town population ranged from 0.45 to 1.59 with an average of 0.74 ± 0.02 mSv/y. The lung cancer cases per year per million person for dwellers in Tammoun town was worked out to be about $(1.25 \pm 0.03) \times 10^{-5}$.

Average radon concentrations for ground and first floor are, respectively, 29.53 ± 0.92 Bq/m^3 and 28.76 ± 1.16 Bq/m^3 while average

radon concentrations for bedroom, sitting room, kitchen and store are: 29.04 ± 0.86 Bq/m^3, 29.43 ± 1.16 Bq/m^3, 28.76 ± 1.81 Bq/m^3 and 31.45 ± 1.03 Bq/m^3, respectively.

All of the above results are low and do not lead to radiation risk to the population.

Chapter One

Introduction

Chapter One
Introduction

1.1. Background:

Ground radiation sources are responsible for most of the human exposure to natural radiation. Although all people are being exposed to natural radiation, some may be exposed more than others according to the area where they live on Earth due to the presence of radioactive rocks or soil in the layers of the earth beneath those areas. The way people live is also affecting the amount of radiation they can be exposed to.

Radon is one of the radioactive elements of the uranium-238 series, but it differs from other elements of the chain as it is a gas. Therefore it can move easily and freely through rocks' cracks and soil pores. It can also enter houses through openings of the land. Houses, especially with low pressure, may work as vacuum pump which pulls emissions from the soil. The risk increases when high amount of gas accumulates and its concentration increases inside buildings. As a result, the cases of lung cancer will increase by inhaling these emissions.

The chemical effects that can damage the cell, especially water molecules that make up most parts of the cell, appear in several forms; the death of the living cell, the prevention or delay of cell division, the increasing of growth rate and its division or the permanent changes in the cell formation genetically during its dividing into subsequent generations (Aggarwal 2014).

This study as many other ones provide information on the concentration of radon indoors and related health risks to dwellers of Tammoun town with the aim of reducing both general population risks and individual risks.

1.2. Literature Review:

There is a large variability in indoor radon concentration levels between different countries, even between areas of the same country, because of differences in the geology of the subsoil, in the climatic parameters and in the building characteristics (Papaefthymiou, 2003).

Also, Radon exposure patterns in large buildings such as schools, commercial buildings and multiunit residential structures may differ from exposure in detached houses due to differences in building structure, occupancy and heating, ventilation and air conditioning operation.

In 2009, WHO published the "WHO handbook on indoor radon: A public health perspective", which provides policy options for reducing health risks from residential radon exposure through establishing a national annual average concentration reference level of 100 Bq/m^3, but if this level cannot be reached under the prevailing country specific conditions, the reference level should not exceed 300 Bq/m^3 (WHO, 2009).

1.2.1. Studies in schools

Several studies have been conducted to find the concentration of radon in different regions of the world, such as in 77 schools of the prefecture of Xanthi in northern Greece. It was found that the radon concentration within it ranged between 45 and 958 Bq/m^3, while the arithmetic mean radon concentration is 231 Bq/m^3 (Clouvas et al., 2009).

Another study performed in 35 secondary schools in the Oke-Ogun area, South-west Nigeria. The average radon concentration for the region was 45±27 Bq/m^3 (Obed et al., 2011).

A number of national studies were carried out in schools to measure radon concentrations, one of which was in four governmental schools for girls in the Tarqumiya town in the northwestern part of Hebron, where the concentration of radon ranged from 12 to 232.5 Bq/m^3 with an average of radon of 34.1 Bq/m^3 and an annual effective dose ranging from 0.62 to 12.0 mSv/y with an average of 1.76 mSv/y (Dabayneh 2006).

Another study was performed in the schools of Tulkarm province, located in the extreme northwest of the West Bank in Palestine. Results of radon concentration ranged, in the classrooms of 20 elementary schools, between 3.48 and 210.51 Bq/m^3 with an average radon concentration 40.42 ± 2.49 Bq/m^3. The average effective annual dose of radon was assessed to be 0.17 ± 0.01 mSv/y while the risk of injury Lifetime excess lung cancer is about 0.09%. (Al-zabadi et al., 2015)

1.2.2. Studies in university buildings

Two studies were performed in two Palestinian universities. The first was in the buildings of Hebron University in 1996, where 54 detectors were used in four buildings, the average radon concentration was 29.8 Bq/m^3 with an average effective dose equivalent of 1.49 mSv/y (Hasan 1996).

The second study was in the buildings of the Arab American University in Jenin during the winter and spring 2014. Radon concentrations and estimated effective dose were found for populations ranging from 26 to 258 Bq/m^3 and 0.69 to 2.12 mSv/y, respectively. The arithmetic mean for indoor radon concentrations and the estimated effective dose average for the population were found equal to 76.6 ± 16.2 Bq/m^3 and 1.15 mSv/y, respectively (Abu-Samreh et al., 2016).

1.2.3. Studies in hospitals and health centers

Measuring radon levels in hospitals is essential to maintaining a healthy environment. Therefore, many studies were carried out within it, such as those that were performed in 28 different buildings at the University Hospital in Bari (Apulia region, southern Italy) for one year divided into two equal periods, where the radon concentration ranged from 6.5 to 388.0 Bq/m^3. The mean annual concentration of radon was expressed in the mean value of 48.0 Bq/m^3. The median value for the period between February and July was 41.0 Bq/m^3 compared to the period between August and January which was 55.0 Bq/m^3 (Vimercati et al., 2018).

As for the studies performed for four hospitals and two health centers in Nablus city in Palestine, an annual effective dose varied between 1.19 mSv/y to 4.60 mSv/y, the average concentration of radon In these hospitals ranged from 23.85 to 92.03 Bq/m^3 and the average of lifetime of radon induced lung cancer was found to vary from $2.41x10^{-4}$ to $9.29x10^{-4}$ (Dwaikat N. 2001).

1.2.4. Studies in homes

In Jazan province in Saudi Arabia, the annual average indoor radon concentration in dwellings varied from (18.2±5.5) to (41.4±10.4) Bq/m^3 with a mean value of (31±6.6) Bq/m^3. The seasonal variations of indoor radon reveal the maximum values in winter and minimum in summer. Mean concentrations amount to 27.4, 35.7 and 31.7 Bq/m^3 in the living rooms, guest rooms and bedrooms, respectively. The annual estimated effective dose received by the residents of the studied area was found to vary from (0.47 ± 0.05) to (1.06 ± 0.14) mSv/y with the mean value of (0.80±0.08) mSv/y. The lifetime fatality risk is found to vary from 0.29 to 0.65% (Amin 2015).

A recent study was conducted in Ainkawa Region in Iraq. The indoor radon concentrations was found to vary from 55.99 to 112.8 Bq/m^3 with an average of 84.30 Bq/m^3, the range of annual effective dose were 1.41-2.87 mSv/y, with average 2.12 mSv/y, and the potential alpha energy concentration range are 6.05 to 12.32 mWL with mean of 9.11 mWL (Hanaa et al., 2018).

In Bingöl and Mus provinces of Turkey, the detectors were placed in the selected 77 dwellings of Bingöl in the 2013 winter season and in 91 dwellings of Mus in 2012 winter season. The estimated values for radon activity concentration are in the range 43 to 348 Bq/m³ with 103 Bq/m³ as a mean value, and from 25 to 604 Bq/m³ with an average of 108 Bq/m³, respectively (Pınar köç et al., 2017).

Also, indoor radon concentration measurement were carried out in Akoko region of Ondo state in Nigeria. The indoor radon concentrations were found to vary from 15.00 Bq/m^3 to 141.00 Bq/m^3 with a mean of 35.54 Bq/m^3 and geometric mean of 29.95 Bq/m^3. Annual exposure varied between 0.10 WLM to 0.17 WLM with an average of 0.13 WLM, annual effective dose varied between 0.38 mSv/y to 0.69 mSv/y with a mean of 0.50 mSv/y and lifetime fatality risk varied between $0.50x10^{-4}$ to $0.85x10^{-4}$ with a mean of $0.64x10^{-4}$ in bedroom, living room, store and lobby (Asere A. M& Ajayi I. R, 2017).

While in the Central Part of Sudan, the radon concentration in the studied towns was found to vary from (86 ± 10) Bq/m^3 in Al-Hasahisa to (66 ± 8) Bq/m^3 in Rufaa. The effective dose rate from $^{222}_{86}Rn$ in the studied towns ranged from (2.18 ± 0.26) to (1.67 ± 0.20) mSv/y and the relative lung cancer risk for radon exposure was 1.078 to 1.059% in Al Hasahisa and Rufaa towns respectively (Elzain 2018).

There are many national studies conducted inside the houses, one of them in Tulkarem province, at Illar region. Indoor radon levels and the

annual effective dose in houses were found to be from 4.9 to 116.0 Bq/m^3 and 0.11 to 1.73 mSv/y, respectively, with average values of 38.3 Bq/m^3 and 0.96 mSv/y. Average values of radon concentration levels in living rooms, bedrooms, bathrooms and kitchens were 14.0, 27.1, 44.45 and 69.3 Bq/m^3 respectively. The corresponding average values of annual effective dose for the living rooms, bedrooms, bathrooms and kitchens were 0.35, 0.68, 1.11, 1.73 mSv/y, respectively (Jazzar & Thabayneh, 2014).

Also, a study reported the seasonal variations of indoor radon levels in dwellings located in the Ramallah province and East Jerusalem suburbs. The study found that the radon concentration levels in summer varied from 43 to 192 Bq/m^3 for buildings in the Ramallah province and from 30 to 655 Bq/m^3 for East Jerusalem suburbs. In winter, the radon concentration levels are found to vary from 38 to 375 Bq/m^3 in the Ramallah buildings and from 35 to 984 Bq/m^3 in East Jerusalem suburbs (Leghrouz et al., 2012).

Another indoor radon measurement was performed in northern part of West Bank, at Tubas town, the neighboring city of Tammoun. The detectors were placed in the selected 87 different rooms during the summer of 2015 using 100 detectors. The results of indoor radon concentrations and the annual effective dose in rooms were found to vary from 48 to 416 Bq/m^3 and 1.2 to 10.4 mSv/y, with average values of 137.0 Bq/m^3 and 3.43 mSv/y , respectively (Abu-Samreh 2017).

1.3. Motivation of research

1. To investigate if there is a radiological environmental hazard inside the selected dwelling in Tammoun town that could be associated with an increase in indoor radon exposure compared with the international permitted exposure limits.

2. To contribute to the creation of a national radon concentration contour map for state of Palestine.

1.4. Study objectives

1. To evaluate the average indoor radon concentration levels inside the selected dwellings in Tammoun town during a three-months period in the summer-autumn seasons.

2. To evaluate the annual effective dose for the population from the indoor radon exposure.

3. To evaluate lung cancer cases per year per million person

4. To compare the average indoor radon concentrations at different geographic sites in Tammoun town.

5. To compare the average indoor radon concentrations at different room (bedrooms, kitchens and living rooms) inside the selected dwellings.

6. To compare the average indoor radon concentrations between different floor levels inside the selected dwellings.

7. To compare indoor radon concentration with those already reported in other Palestinian locations.

8. To assess the safety of these buildings in terms of radiation and if necessary take the necessary remedial actions to reduce the radon levels in these buildings.

Chapter Two
Concepts of Radioactivity

Chapter Two

Concepts of Radioactivity

2.1. Introduction to Radioactivity

Radioactivity is a natural phenomenon, so that the unstable nuclei emit particles or electromagnetic energy to reach stable nuclei.

Henry Becquerel observed the radioactivity in 1896 by chance. Some experiments studied the ability of uranium salts to absorb the light falling on them and then use it's emitted light to test their fiuresescence. But when he placed these salts near a film inside his dark cabinet, he noticed that the film is affected by light (Allisy, 1996).

Marie Curie then began studying all the elements available to her at Sorbonne University to test their emissions. Noting that some emissions of thorium salts are similar to emissions from uranium salts. But a German scientist, Gerhardt Schmidt, found the effect of thorium salts on the photographic plate, two months before Marie Curie did. However, Marie Curie, is the first to call the emissions from unstable nuclei " radiation activity", she was able to discover two new elements, radium and polonium, moreover she won the Nobel Prize in Physics in 1903 with her husband for their work in radioactivity (Adloff, 1999).

2.2. Patterns of Nuclear Stability

Although protons have a positive charge, the protons remain coherent within the nucleus. This is due to the nuclear force, which is stronger than

the electrostatic force between the protons, where this force is between all nucleons (protons and neutrons).

Therefore, the stability of nuclei is based on the study of nucleons inside the nucleus, and the study of interconnection force between them.

2.2.1. Neutron to proton ratio

There are several observable factors working on the stability of the nucleus, the most important one is the ratio between the number of neutrons to protons (N/Z), where if we draw the number of neutrons versus the number of protons for all known nuclei we get the result shown in (Figure 2.1) (Choppin et al., 2001).

We conclude that the most stable nuclei are in which (N/Z) equal one and where the number of protons ($Z<20$), whereas for the nuclei in which the number of protons ($20<Z<82$), the ratio between neutrons and protons is increases slowly from 1 to 1.5. Finally, all nuclei with the number of their protons ($Z>82$) are unstable.

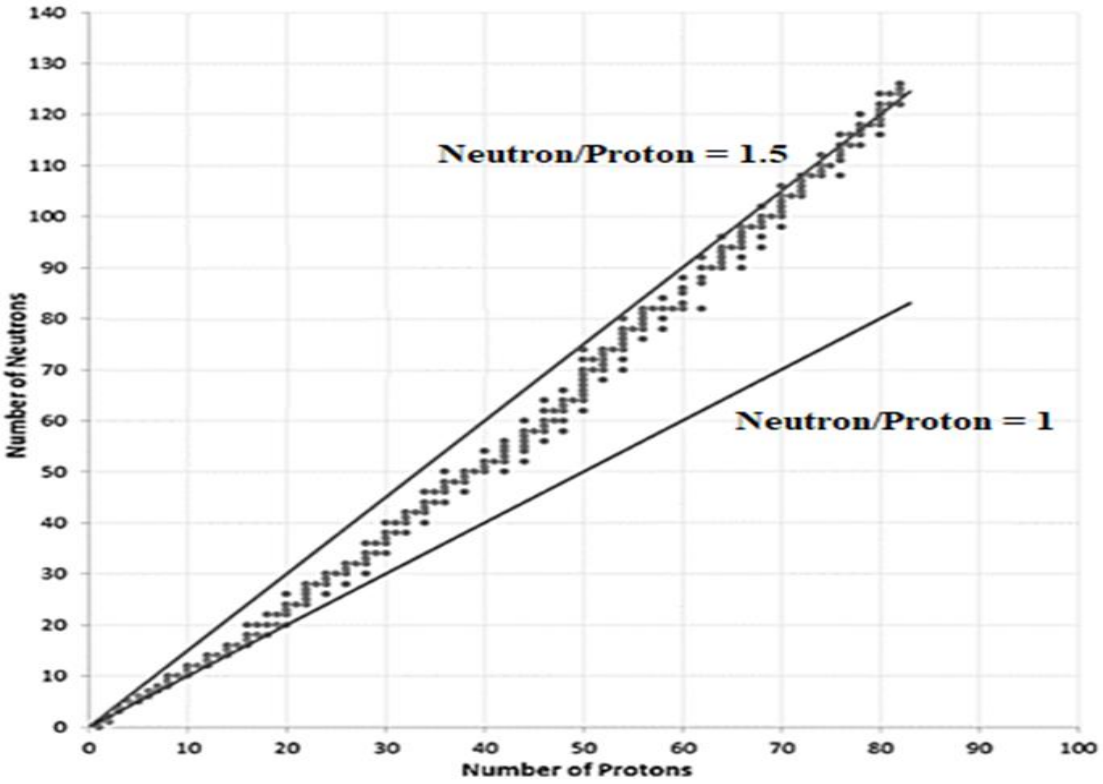

Figure 2. 1 A plot of the number of neutrons against the number of protons.

2.2.2. Even odd effect

Another factor causes the stability of the nucleus, where nuclei with even number of protons and neutrons are the most stable. Figure (2.2) shows that the number of stable nuclei is large when the number of protons and neutrons is even, while the number is small when both are odd.

This can be explained by the fact that nuclear force is greater when the nucleon is paired with another nucleon (Vertes et al., 2006).

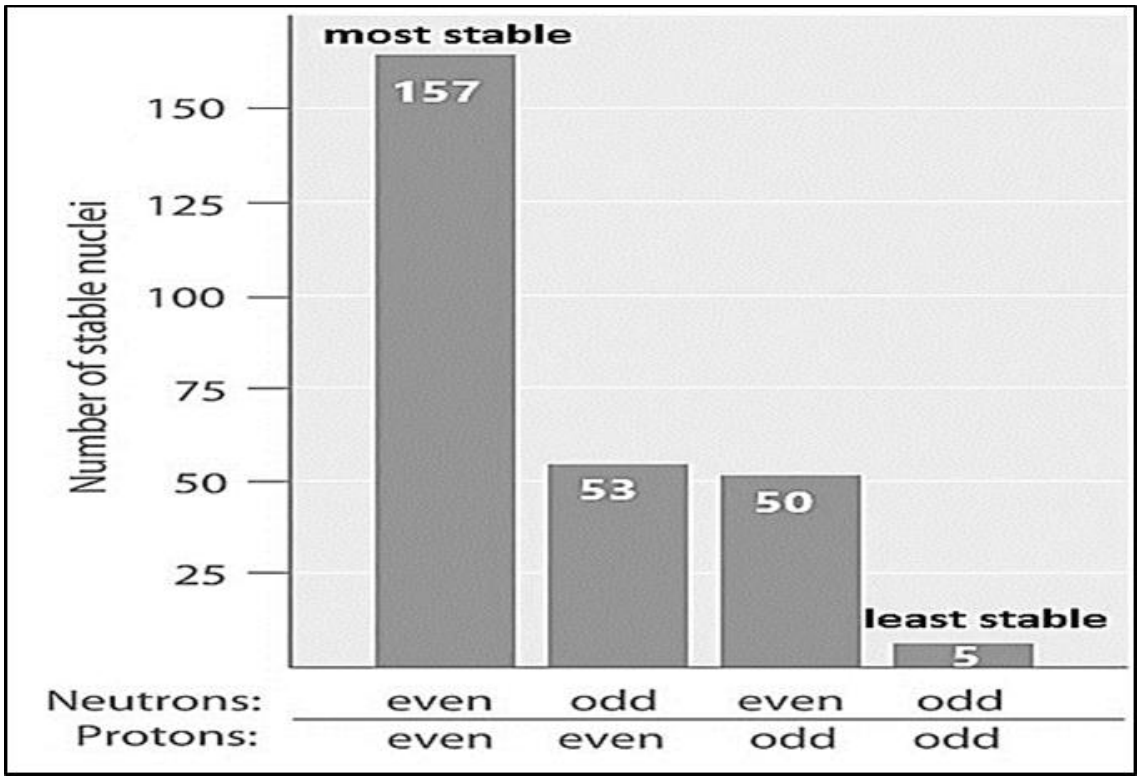

Figure 2. 2 Number of stable nuclei with even and odd numbers of protons and neutrons

2.2.3. Magic numbers

In addition, there are specific pairs of protons and neutrons that lead to greater stability of the nucleus. These numbers are (2, 8, 20, 28, 50, 82, 126) which are called magic numbers (Raymond et al., 2004).

The nucleus is stable when the number of protons or neutrons in it is one of these numbers. The nucleus is more stable when the number of protons and neutrons in it is one of these numbers.

2.2.4. The binding energy (BE) per nucleon

The nuclear bonding energy of each nucleon is one of the factors by which the stability of the nucleus can be predicted. As the bonding energy of each nucleon increases, the stability of the nucleus increases.

The nuclear bonding energy per nucleon can be found using the following equation:

$$\text{BE/nucleon} = \frac{[(Nm_n + Zm_p) - M]C^2}{A} \qquad (2.1)$$

where:

C is the speed of light, m_p is the mass of proton, m_n the mass of neutron and A is the number of nucleons in the nucleus.

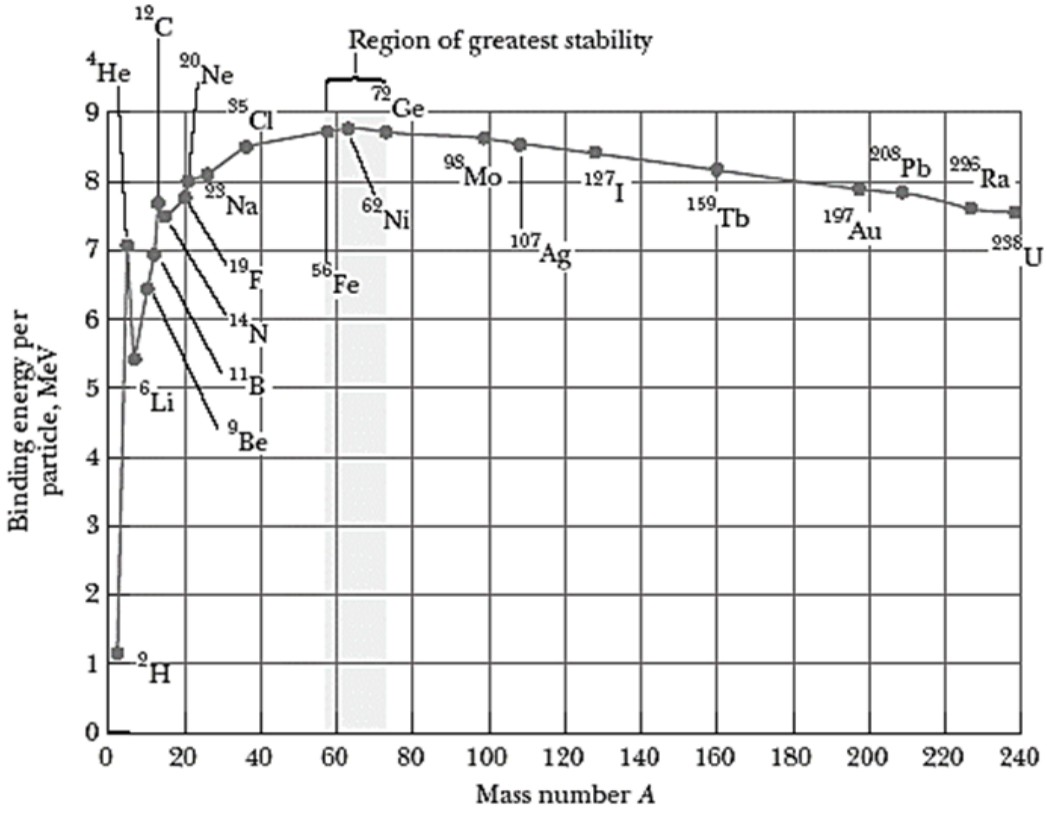

Figure 2. 3 Binding energy curve

Therefore, using Figure 2.3, we observe the following:

1. The most stable elements are nickel and iron isotopes where the binding energy of each nucleon is 8.8 MeV.

2. The elements at both ends of the curve seek to reach stability through nuclear fission or nuclear fusion. Heavy nuclei such as uranium have nuclear fissionability if the right conditions exist, producing more stable nuclei and nuclear bonding energy for each nucleon is larger than the parent nucleus. Light nuclei undergo nuclear fusion if they have the right conditions, so that the nuclear energy of each nucleon of the resulting nucleus becomes larger than the nuclei combined (Diwan 2014).

2.3. Types of decay

In the definition of radiation we have mentioned that nuclei in nature seek to achieve stability by emitting particles called alpha particles and beta particles and can emit electromagnetic energy as gamma radiation. Therefore, the properties of the nuclear radiation resulting from the decay can be identified in (Table 2.1).

Table 2. 1 shows the properties of nuclear emissions (α.β.γ).

Radiation type	α	β^-	β^+	γ
Physical nature	Helium nucleus	Electrons	Positrons	Photons
charge	+2	-1	+1	0
Rest mass in (a.m.u)	4.001506	0.000549		0
Speed	0.1 C	0.99 C		C
The ability to ionize	High	Medium		Low
The ability to penetrate	Low	Medium		High
Stopped by	Paper	Thin aluminum sheet		Lead

The following diagram (Figure 2.4) show the effect of electric and magnetic fields on the Radiation types, where it shows gamma radiation in a straight line without deviating; because it does not have a charge. Nuclear radiation $(\alpha.\beta.\gamma)$ will be discussed briefly in this section.

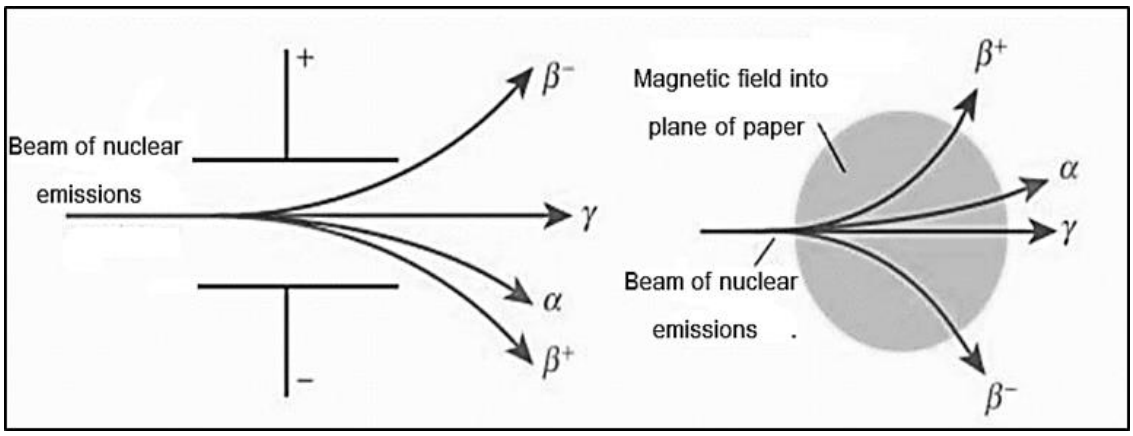

Figure 2. 4 Effect of electric and magnetic field on nuclear emissions.

2.3.1. Alpha decay

It is known that heavy nuclei (Z > 82) are less stable; because the electrostatic force between protons becomes larger than nuclear force. Therefore, the nuclei emit alpha particle radiation in addition to another new are more stable nucleus, and is called a daughter. The alpha-radiation formula can be written as follows:

$$X_Z^A \quad \rightarrow \quad Y_{Z-2}^{A-4} \quad + He_2^4 \qquad (2.2)$$

Where element X represents a heavy nucleus called parent, while element Y represents the resulting new nucleus called daughter in addition the helium nucleus which is called the alpha particle.

The energy of alpha particles varies depending on the parent nucleus, so it has constant energy for each nucleus.

Figure 2.5 represents the relationship between the different energies of alpha particles and the range in the air. The particle's range is the distance covered from the moment the body emits during decay to its stoppage, which depends on the material through the body and particle energy passed at the moment of decay.

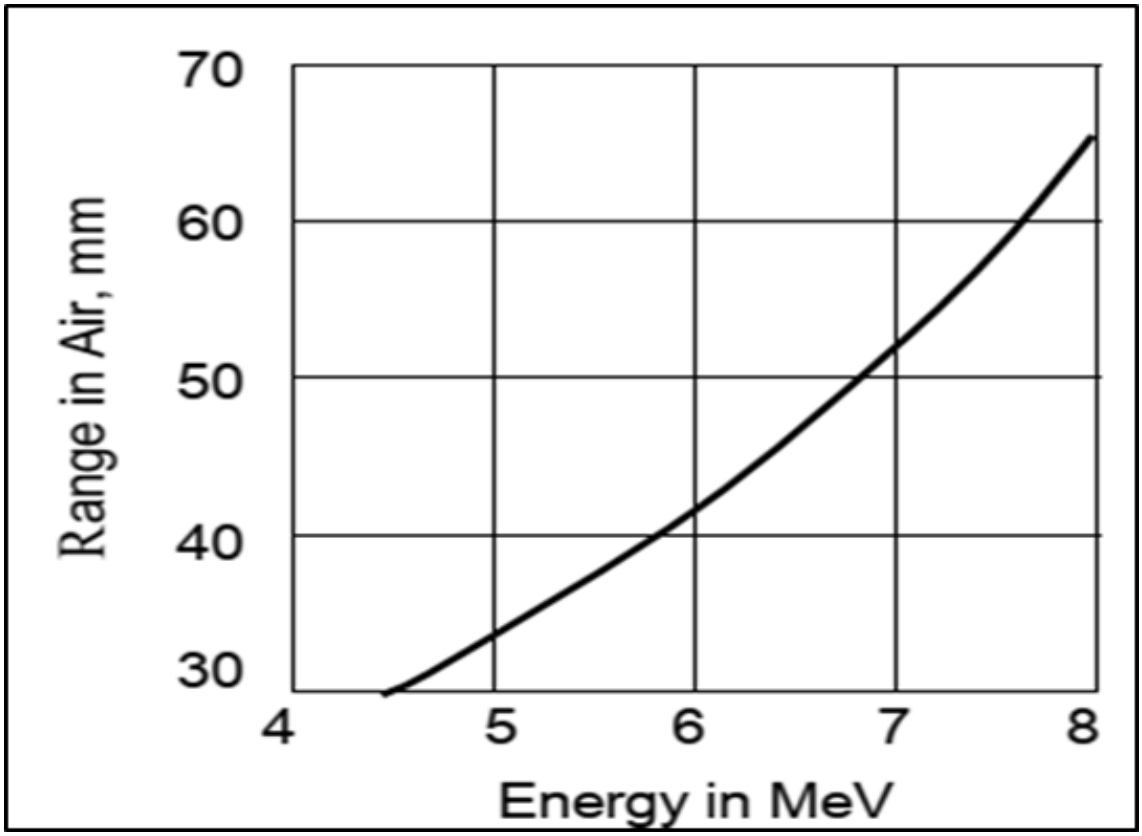

Figure 2. 5 Energy of alpha particle vs. the range in the air.

Therefore, the effect of alpha particles on the human body from the outside is almost non-existent, because it cannot penetrate the skin of the human body, but these particles become dangerous if it enters into the human body (Burnham 2011, Smith 2014).

2.3.2. Beta decay

Beta particles are fast electrons or positrons emitted by the decay of nucleons in nuclei that contain excess of proton and neutron respectively.

Although beta particles can penetrate some body tissues more than alpha particles, the damage of alpha particles inside the body is greater; because of their high ionization potential.

Beta particles also differ from alpha particles because one radioactive element is capable of emitting beta particles with different energies. The average energy is equal to one third of the maximum energy emitted, and the maximum energy of most beta particles is between (0.1- 4) MeV (Magill & Galy 2005).

It appears from Figure 2.6 that high density materials have a greater ability to block beta particles. The types of beta particles are discussed below.

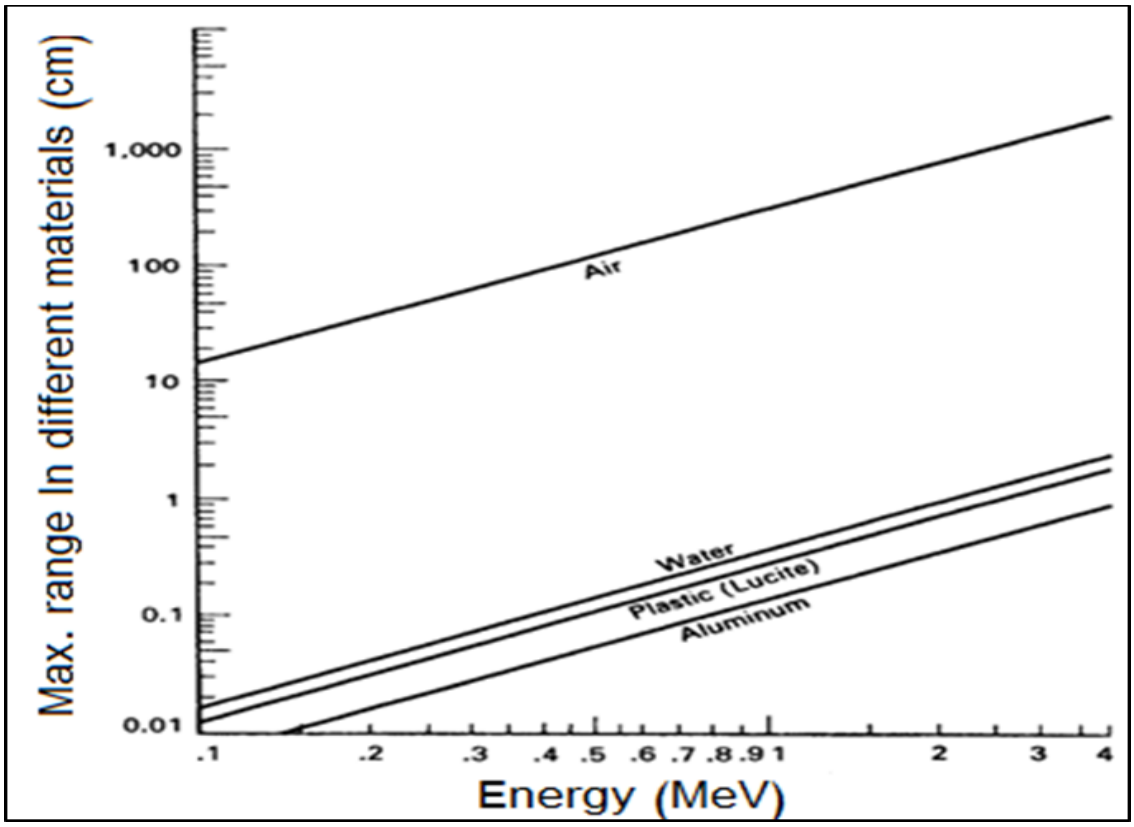

Figure 2. 6 Energy of beta particle vs. the range in different materials.

2.3.2.1. (β^-- decay):

This emission occurs when the ratio between neutrons and protons becomes greater than one, so these nuclei release an electron as well as a subatomic particle called the antineutrino "$\bar{\nu}_e$". In beta decay, conservation laws are in place so an antineutrino is released in the decay to keep the energy, angular momentum (spin) and linear momentum conserved. The antineutrino has no mass and does not carry an electrical charge (Raymond et al., 2004).

The general formula for decay of negative beta particles can be written as follows:

$$_{Z}^{A}X \rightarrow {}_{Z+1}^{A}Y + {}_{-1}^{0}e + \bar{\nu}_e \qquad (2.3)$$

2.3.2.2. (β^+- decay):

This emission occurs when the ratio between protons and neutrons becomes greater than one, so these nuclei release positrons, the antiparticle of the electron as well as a subatomic particle called the neutrino "υ". The positron is a particle that has the same electron mass and the same amount of charge but differs in the sign of charge.

The decay of positive beta particles occurs by the following general formula:

$$ {}^{A}_{Z}X \rightarrow {}^{A}_{Z-1}Y + {}^{0}_{+1}e + \upsilon_e \qquad (2.4) $$

2.3.2.3. Electron capture

Is a process that occurs when an electron in the inner orbits of the nucleus unites with a proton to produce a neutron in addition to neutrino by the following equation:

$$ {}^{A}_{Z}X + {}^{0}_{-1}e \rightarrow {}^{A}_{Z-1}Y + \nu_e \qquad (2.5) $$

After the capture of electron from the inner orbit of the atom, electron starts moving from the outer orbits to fill the vacancy and so on. This movement of electrons leads to X-ray emission.

2.3.3. Gamma decay

The nucleus radiates gamma rays when the nucleus is excited. This state of the nucleus occurs either as a result of a nucleus collision that is violent with another nucleus or as a result of alpha or beta decay.

The general formula for Gamma decay can be written as follows where X^* indicates a nucleus in an excited state:

$$^{A}_{Z}X^* \rightarrow {}^{A}_{Z}X + {}^{0}_{0}\gamma \quad (2.6)$$

Gamma rays have high energy, ranging from 0.1 to 10 MeV. This means that they have a short wavelength of between 0.1 and 140 pm. Therefore, to stop gamma rays, materials such as lead which has a high atomic number and high density is used.

2.4. Radioactive decay

It is impossible to predict the time of one nucleus decay, while the probability of decay of a sample containing a group of nuclei can be statistically predicted. This is because the decay process is a random process that happens to the nucleus spontaneously without relying on physical properties (such as temperature and pressure).

2.4.1. The Radioactive decay law

If the number of radioactive nuclei in a sample is N at time t, the number of radioactive nuclei will decrease by the number of decayed nuclei dN after dt time.

The radioactive decay constant, λ, is defined by equation (2.7) as:

$$\lambda = \left(-\frac{\left(\frac{dN}{dt}\right)}{N}\right) \quad (2.7)$$

Equation (2.7) is then integrated as follows

$$\int_{N_0}^{N_t} \frac{dN}{N} = -\lambda \int_0^t dt \qquad (2.8)$$

Finally we get the exponential decay law

$$N_t = N_0 e^{-\lambda t} \qquad (2.9)$$

N_0 the number of radioactive nuclei at t = 0 and N_t the number of nuclei remaining after a period of time (t). While the negative sign in equation (2.7) indicates decreasing in the number of nuclei as a result of decay (Smith 2014, Raymond et al., 2004).

2.4.2. Activity

Activity or called the decay rate (R) is the number of decays per unit time, it represents ($\frac{dN_t}{dt}$) so that it can be written:

$$R = \left|\frac{dN_t}{dt}\right| = N_0 \lambda e^{-\lambda t} = R_0 e^{-\lambda t} \qquad (2.10)$$

Where R_0 is the decay rate at (t = 0) .

2.4.3. Half-life:

The period of time required so that half of the original number of nuclei (N_0) of the radioactive element decay so that the number of remaining nuclei becomes ($N_t = \frac{1}{2} N_0$) when the time

($t = t_{1/2}$). Putting it in equation (2.9) to get:

$$t_{1/2} = \frac{\ln(2)}{\lambda} \qquad (\mathbf{2.11})$$

2.5. Radioactive decay series

There are three chains of natural radioactive decay. All chains start with an unstable element, half-life of which is greater than the elements that follow in the chain, all ending with lead isotopes as shown in figure 2.7. These chains are:

1. 1\ Uranium Series, begins with uranium isotope ($^{238}_{92}U$) and ends with lead isotope ($^{206}_{82}Pb$).

2. 2\ Actinium Series, begins with uranium isotope ($^{235}_{92}U$) and ends with lead isotope ($^{207}_{82}Pb$).

3. 3\ Thorium Series, begins with Thorium isotope ($^{232}_{90}Th$) and ends with lead isotope ($^{208}_{82}Pb$).

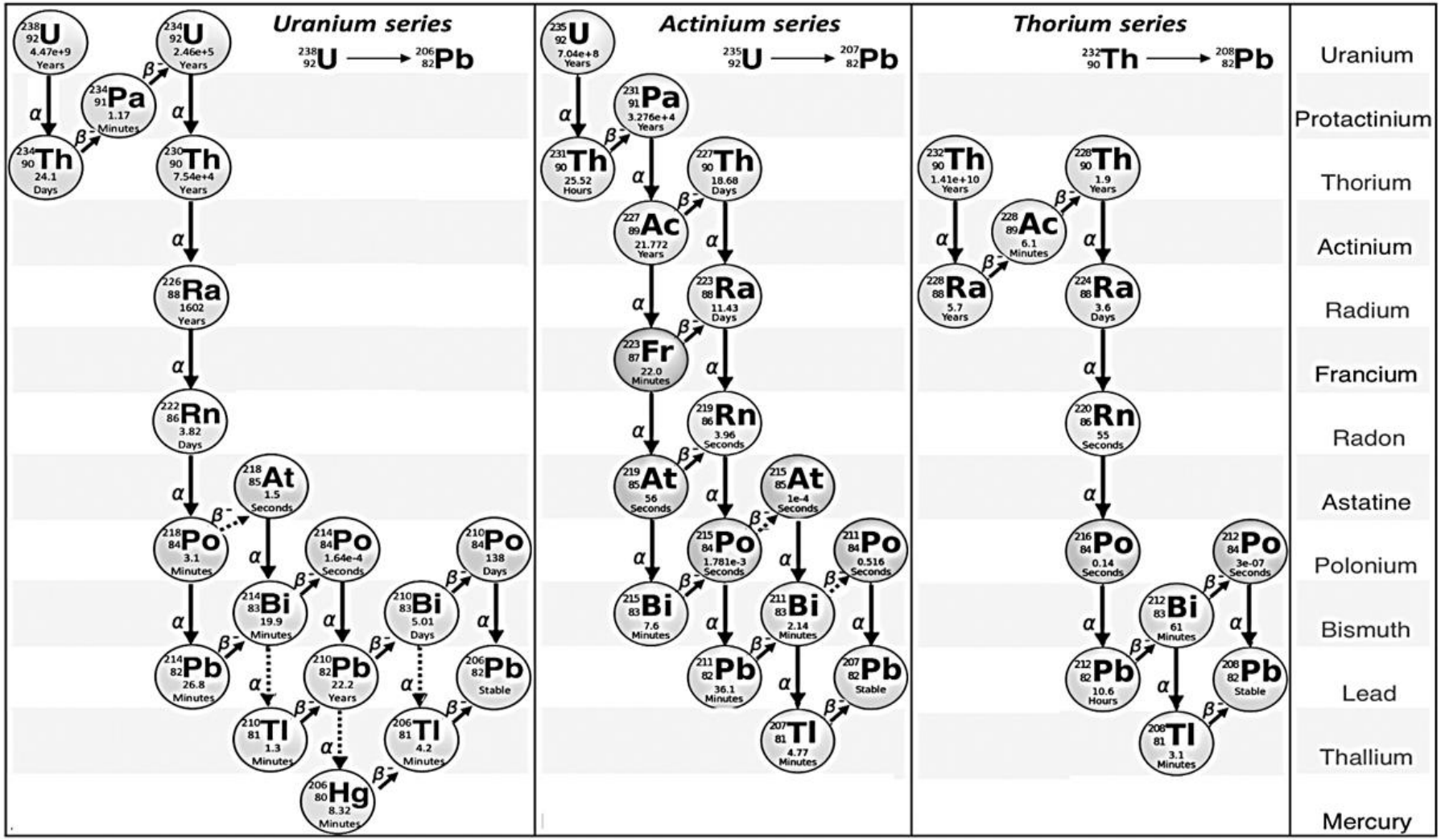

Figure 2. 7 The three chains of natural radioactive decay

Additionally, there is a series called neptunium series, the half-life of the nucleus at the beginning is much less than Earth's age, which means that this series is not present in nature, but can be produced in laboratories. It starts with element ($^{237}_{93}Nb$) and ends with element ($^{209}_{83}Bi$).

2.6. Radiation units

Radiation units are many and different, so they are divided into four main parts, each part containing a set of those units

2.6.1. Radioactivity units

1. Becquerel (Bq):

One Becquerel is defined as one decay per second. It is the international measurement unit of radioactivity.

2. Curie (Ci):

One Curie equals the number of decay caused by a gram of radium ($^{226}_{88}Ra$) per second. Where 1Ci = $3.7 \times 10^{10} Bq$.

2.6.2. Radiation exposure unit

Radiation exposure is defined as the amount of ionization per unit mass that occurs to the matter due to nuclear radiation, measured by Roentgen.

Roentgen (R):

The Rontgen is equivalent to ionizing charges of 2.58×10^{-4} Coulomb in one kilogram of air($1R = 2.58 \times 10^{-4} C/Kg$).

2.6.3. Absorbed dose units

The absorbed dose is equivalent to the amount of energy deposited from ionizing radiation per unit of mass from the matter. The SI unit for measuring the absorbed dose is the Gray (Gy).

1. Gray (Gy):

One Gray is equivalent to the absorption of one joule of ionizing radiation energy by one kilogram of matter.

2. Radiation absorbed dose (Rad)

One rad is equivalent to the absorption of (100 erg) of ionizing radiation energy by one gram of matter.

1 rad = 0.01 Gy

2.6.4. Radiation protection unit

There are two types, the equivalent dose which depends on the type of radiation. The second is called effective dose and depends on the type of organ or tissue that is affected by radiation, all measured by the Sievert (Sv) unit.

2.6.4.1. Equivalent dose

The equivalent dose is intended to obtain the same degree of damage that different types of radiation can cause to the organism. Each type of radiation has a different harm, so each type has a radiation

weighting factor (w_R), given in table 2.2, when multiplying it by the absorbed dose produces the equivalent dose.

2.6.4.2. Effective dose

Each tissue in the organism's body is affected by radiation in a different way. To find the Effective dose we multiply the amount of energy absorbed by the tissue weighting factor ($\boldsymbol{w_T}$).

Table (2.3) shows the tissue weighting factor for some organs and tissues of the body.

So the one Sievert equivalent to one gray dose absorbed from the radiation of beta particles ($\boldsymbol{w_R}$ for beta particles equals 1), or the one Sievert equivalent to 100 gray dose absorbed by the skin ($\boldsymbol{w_T}$ for skin equals 0.01). Another unit used is Roentgen equivalent man (Rem), Rem is equivalent to 0.01 Sv where the dose absorbed by the unit rad.

1 rem = 0.01 Sv

Table 2. 2 Radiation weighting factor for each type of radiation (ICRP 1991)

Type of radiation	**Energy range**	**weighting factor ($\boldsymbol{w_R}$)**
Photons, electrons	All energies	1
Neutrons	<10 keV	5
	10-100 keV	10
	0.1-2 MeV	20
	2-20 MeV	10
	>20 MeV	5
Protons	<20 MeV	5
Alph particle, fission		
Fragments, heavy nuclei		20

Table 2. 3 The tissue weighting factor for each type of radiation (ICRP 1991)

Tissue	weighting factor w_T	**Tissue**	weighting factor w_T
Gonads	**0.2**	**Liver**	**0.05**
Red bone marrow	**0.12**	**Oesophagus**	**0.05**
Colon	**0.12**	**Thyroid**	**0.05**
Lung	**0.12**	**Skin**	**0.01**
Stomach	**0.12**	**Bone surface**	**0.01**
Bladder	**0.05**	**Remainder**	**0.05**
Breast	**0.05**		

2.7. Effects of radiation

Ionizing radiation damage depends on several different factors, the equivalent dose, the effective dose, the dose rate, the age of the person exposed to the radiation, etc. Damage to humans has been studied following the follow-up of victims and survivors of nuclear accidents, uranium miners, radiologists and patients exposed to radiation.

The physical effects of exposure to radiation may occur immediately within hours or may occur gradually for a long period of several years. The following table (2.4) shows some early effects that appear with varying absorbed doses.

Effects may appear after along exposure to low doses for prolonged periods such as cancer, fibrosis in various tissues and cataract of the eye lens (Aggarwal 2014).

Because of radiation damage, annual dose limits should be set so that they do not affect people if exposed to them.

Table (2.5) represents the dose limits allowed by the International Commission on Radiation Protection (ICRP) 1991

Table 2. 4 Some early effects that appear with varying absorbed doses.

Dose Range	Immediate Effect	Notes
Less than 0.1 Gy	no detectable effects	
Above 0.5 Gy	Decrease in granulocyte count	
Above 1 Gy	Low number of lymphocytes and radiation sickness in the form of nausea and vomiting	exposed person recover after one or two days
Above 3 Gy	irrecoverable damage occurs to the blood forming organs	
3-5 Gy	Hematopoietic Syndrome	about 50% of the exposed persons may die within 60 days
7-10 Gy	Gastrointestinal Syndrome	Death occurs in 7 to 14 days time
Above 10 Gy	consequences of damage to central nervous system manifest	
Above 25 Gy	Central Nervous System Syndrome	Death occurs in 1 to 2 hours time

Table 2. 5 The dose limits allowed by the (ICRP 1991) for employees and public.

	Employees (mSv)	**Public (mSv)**
Effective dose	20	1
Equivalent dose		
Lens of the eye	150	15
Skin, hands, forearms, feet, ankles	500	50
Abdomen of woman of reproductive capacity	13	–
Fetus of pregnant employee	1	–

Chapter Three

Radon and methods of measuring its concentration

Chapter Three

Radon and methods of measuring its concentration

3.1. Radon and its isotopes

In 1900, during the study of decay of radium by the German scientist Friedrich Ernst Dorn, radon was discovered. Radon is a radioactive gaseous element in nature. It is one of the most important sources of naturally ionizing radiation to which humans are exposed, about 50% of the radiation dose that humans are exposed to from natural sources of radiation is from radon (Appleton 2013).

It is odorless, invisible, and tasteless, therefore cannot be detected with the human senses.

The density for radon is 8 times greater than the air density, It is one of the densest substances that remain a gas under normal conditions (density = 9.73 Kg/ m^3). Therefore, its concentration is very high in enclosed rocky places such as caves, basements beneath houses, mines and ancient archaeological tombs.

Radon $^{222}_{86}$Rn belongs to the series of decay of uranium $^{238}_{92}$U ($t_{1/2} = 4.5 \times 10^9$y), which has several natural isotopes, the most important of which are the thoron $^{220}_{86}$Rn which belongs to the series of decay of thorium $^{232}_{90}$Th ($t_{1/2} = 1.4 \times 10^{10}$y) and action $^{219}_{86}$Rn, which belong to the series of decay of uranium $^{235}_{92}$U ($t_{1/2} = 7.04 \times 10^8$y) (Mook & Vries 2001).

The effect of actinium is disregarded for two reasons: uranium isotope $^{235}_{92}$U is rare in nature and the other is due to the half-life of actinon ($t_{1/2} = 3.92$ sec).

The rate of production of the thoron and radon through decay within Earth's layers is almost equal, although the amount of thorium in the earth is greater than uranium because the half-life of thorium is greater. However, the thoron effect is smaller because the half-life is short ($t_{1/2} = 55.6$ sec).

Therefore, interest in the study of radon is greater because of the large half-life ($t_{1/2} = 3.82$ d) compared to its isotopes and its ability to penetrate the Earth's layers and reach the air (ATSDR 2012).

3.2. Radon in soil, water, and air:

The following is an explanation of where the radon gases appear in the environment:

3.2.1. Radon in soil

Radon moves through the cracks of rock and soil pores, before it decays to its daughters and settles in the soil.

Soil porosity and moisture content affect the ease of movement of radon, where radon moves more easily through gravel and coarse sand in contrast to clay soils.

Radon concentration ranges between 2×10^3 and 10^6 Bq/m^3 at a depth between 0.5 and 1 m below the soil surface. This range is selected for

depth to increase the validity of the results, where radon concentration is increased relatively rapidly in this range, and a decrease in depth leads to a change in concentration due to the impact of weather conditions.

To calculate the concentration of radon $\boldsymbol{C(z)}$ in depth (z) under the soil surface using equation:

$$C(z) = C_{\infty}(1 - e^{\frac{z}{L_r}}) \quad \text{(3.1)}$$

Where: $\boldsymbol{L_r}$ is the radon diffusion length (m) depend on soil type and $\boldsymbol{C_{\infty}}$ is the radon concentration at large depth of the residue repository (>2 m) (ICRP 2014, IAEA 2013)

3.2.2. Radon in water

In the United States, 11% of stomach cancer patients were found to be consuming water containing a high concentration of radon, according to the report of the National Academy of Sciences.

Therefore, the environment protection agency (EPA) recommended that the concentration of radon in drinking water should be less than 11.1 Bq/L. While the European Union has set guidelines for determining the concentration of radon in water for human consumption ranging from 100 to 1000 Bq/L (Kasić et al., 2016).

3.2.3. Radon in air

When radon succeeds in finding its way into the air, its concentration is reduced due to its mixing with the air components. Radon concentration decreases as we rise from the Earth's surface because it is a heavy gas.

Also, radon concentration in the air over the surface of the ocean is reduced to 0.1 Bq / m^3 due to the radon's ability to solubility in water at low temperatures.

The reason for the increased concentration of radon in indoor buildings is due to factors such as lack of ventilation, level of floor in the building, design of buildings and changing seasons of the year, where radon concentration is greatest possible at night and during winter.

The sources of radon inside the building are:

1. Soil components under the building and building materials where they contain a small concentration of radium, the figure (3.1) represents the ways in which radon enters buildings.

2. Outdoor air increases the concentration of radon inside homes,

3. Water used in homes contains dissolved radon gas that is released in the air of the house. Radon concentration in surface water differs from groundwater where groundwater contains more dissolved radon if used directly.

4. Natural gas used in the kitchen and heating is likely to be mixed with radon while it is present in the Earth's layers, but its contribution to increase concentration is small (ICRP 2014, Nero et al., 1990).

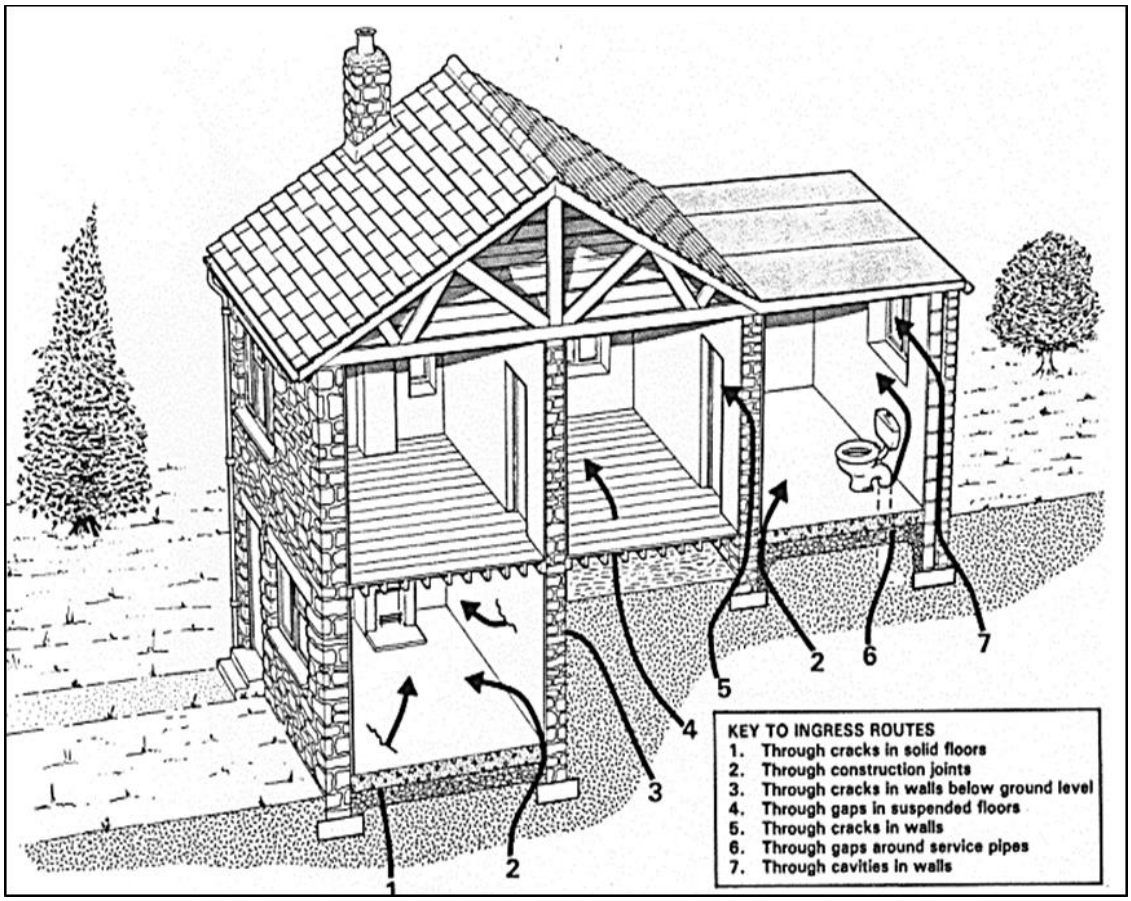

Figure 3. 1 Pathways of indoor radon

3.3. Radon risk

Radon gas enters the human body by inhalation or ingestion, The lung receives the largest amount of this gas. This was evident in studies of the types of cancers suffered by miners, where lung cancer was found to be the highest (ICRP 2010).

The effect of radon starts when it decays to produce its daughters such as polonium isotopes $^{218}_{84}\mathrm{Po}\left(\mathrm{t}_{1/2} = 3.11\ \mathrm{min}\right)$ and $^{214}_{84}\mathrm{Po}$ $(\mathrm{t}_{1/2} = 164\ \mu\mathrm{sec})$, which are in solid state, that settle in the airways of the respiratory system. Also, polonium isotopes $^{218}_{84}\mathrm{Po}$ and $^{214}_{84}\mathrm{Po}$ decay and

release alpha particles with an energy of 6 MeV and 7.69 MeV respectively, with the ability to penetrate fluid or tissues for 48 μm and 71 μm respectively.

Energy interacts with the target, causing damage depending on the amount of energy and the thickness of the protective layer of the cells through which it must pass to hit the sensitive cells. When a cell is infected with an alpha particle, chemical damage to the surrounding water molecules or damage to the DNA through its structure, function or replication, the infected cell then sends a message to the surrounding cells contributing to the formation of the tumor (National Academy of Sciences 1991).

3.4. Radon measuring devices

Radiation can not be sensed or seen but can be monitored by special devices that depend on physical and chemical changes.

Radon concentration varies with time as in figure (3.2) depending on the behavior of the occupants of the dwelling, change of ventilation or weather. For example, if the window of the room is open during a short-term study, this means that the radon concentration will be low in that period, therefore have a low concentration average. So, the long-term study is more accurate because it takes daily changes to radon concentration with attention.

Devices used to measure radon in the air as shown in the table (3.1) are divided into two parts: active devices and passive devices.

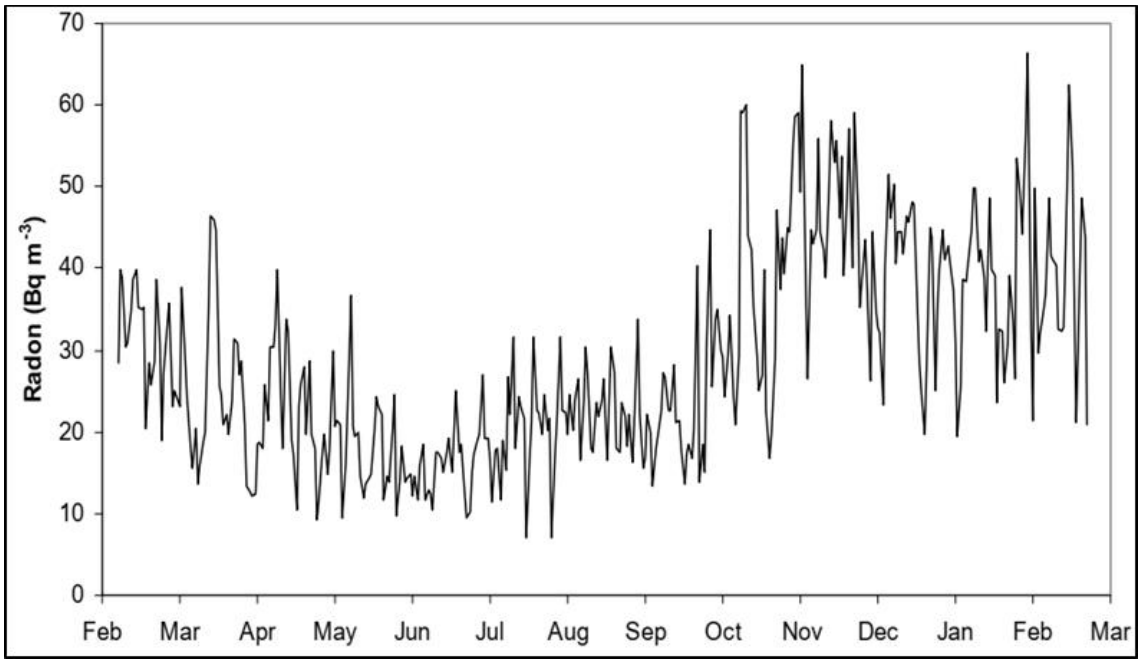

Figure 3. 2 Radon concentration with different months

Table 3. 1 Devices used to measure radon in the air

Type	Characteristics	Example
active devices	They require electrical power a pump to work in the sampling setting. They include the ability to chart the concentration and fluctuations of radon gas during the measurement period	Continuous radon monitors
passive devices	They do not require electrical power a pump to work in the sampling setting	Charcoal canisters. Electret ion chamber detectors Alpha-track detectors

3.4.1. Active devices

3.4.1.1 Continuous radon monitors

There are several types of this detector, some using scintillation cells for measurement, while others use ionization chambers. The gas enters the

device by air diffusion or through a pump, this detector has a counting screen, to monitor the radon concentration change during the measurement period ranging from 2 to 7 days. This means that an electrical power supply is required to operate the device (Gerorge 1999).

3.4.2. Passive devices

3.4.2.1. Activated charcoal detector

Activated charcoal can absorb radon and when radon decays, its daughters are retained, gamma radiation is emitted from $^{214}_{82}Pb$ and $^{214}_{83}Bi$, and by measuring the emitted spectrum the radon concentration can be determined.

Another method of measurement can also be used, by mixing activated charcoal, which is exposed to radon gas with a liquid scintillation cocktail. Radon concentration can be calculated by standard liquid scintillation counting equipment.

Activated charcoal is used for measurement between 48 hours and 7 days and then sent to the laboratory to find the concentration before the gamma radiation activity decreases (Miles 2004).

3.4.2.2. Electret ion chamber detectors

Radon gas enters the ionization chamber through the filter without its daughters by passive diffusion. Then radon decays and the decay chain continues to produce ionizing radiation for the air inside the ionic chamber.

The positive electret, installed at the bottom of the chamber, captures negative ions that are related with radon concentration.

There are long-term ionization chambers that can be deployed for a period of 1 to 12 months, and can be used for short-term if the concentration of radon is high. Other chambers are only used for short-term deployment period ranging from 2 to 15 days (Gerorge 1999).

3.4.2.3. Nuclear track detector

Type of nuclear track detector

The solid-state nuclear track detectors (SSNTD's) (also known as the etched track detector) is one of the most widely used, cheapest and simplest tools. The principle of its action is to record track of heavy charged particles falling on the detector surface that have ($Z \geq 1$).

SSNTDs are divided into three main sections:

1. Crystalline Solids such as Muscovite Mica, Apatite, Olivine, etc.
2. Glasses are divided into two parts: Natural Glasses and Man-Made Glasses
3. Plastics comprises more than 30 species, the most important of which is CR-39 (polyallyldiglycol carbonate (PADC)), Lexan (polycarbonate (PC)) and LR-115 (cellulose nitrate (CN)).

These three type are called Alpha-track detectors. CR-39 is one of the most widely used and sensitive detectors, which can detect alpha particles with energy between 0.1 and 20 MeV. The LR-115 is less sensitive than the CR-39 as it can detect alpha particles with energy between 1.2 and 3.9 MeV. Lexan has a lower sensitivity than the LR-115, which can detect alpha particles with energy between 0.2 and 3 MeV.

The time required to deploy these detector to find radon concentration ranges from 1 to 12 months (L'Annunziata 2012).

Tracks formation and Chemical etching

This topic will be discussed for CR-39 detector due to its use in this study.

Initially, the size and shape of the track give information about the velocity, energy and direction of the alpha particle. The track shape is circular if the particle enters perpendicularly, whereas if it enters otherwise, the mouth of the hole is elliptical. The track diameter varies between 30 and 100 A°.

CR-39 has a long molecular chain, as in figure 3.3, which facilitates its response to path formation. When alpha particles drop at least 2 eV, they break down molecular bonds along their path and continue to break them until they lose their energy, as shown in figure 3.4.

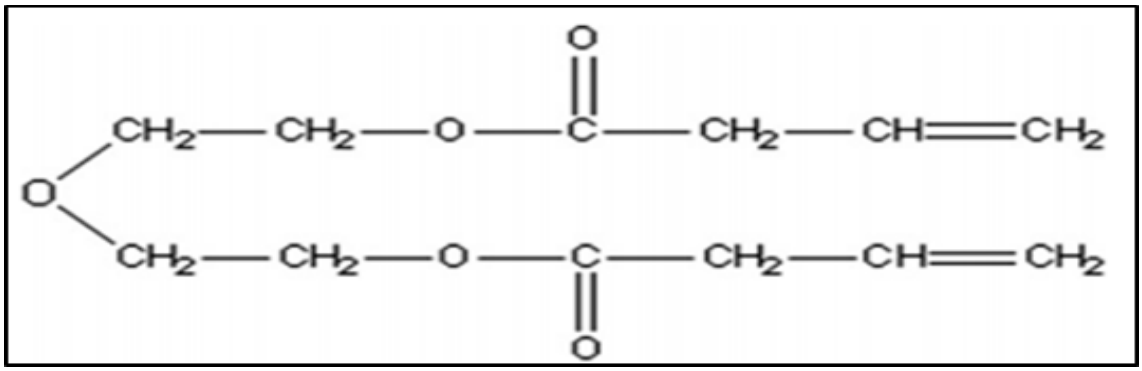

Figure 3. 3 The structure of CR-39

Through the chemical etching process the open ends of the chain are attacked, which leads to the enlargement of the latent track and thus the ability to observe them under an optical microscope.

Figure (3.5) shows the effect of the chemical etching process on the detector.

Three factors must be considered for the chemical etching process to occur correctly: Etching solution concentration, temperature and etching duration.

Therefore, sodium hydroxide solution is used at a concentration of 6.25 M at a temperature of 70 C during a time of 6 hours, the time period can be changed by changing the temperature or concentration of the solution (L'Annunziata 2012).

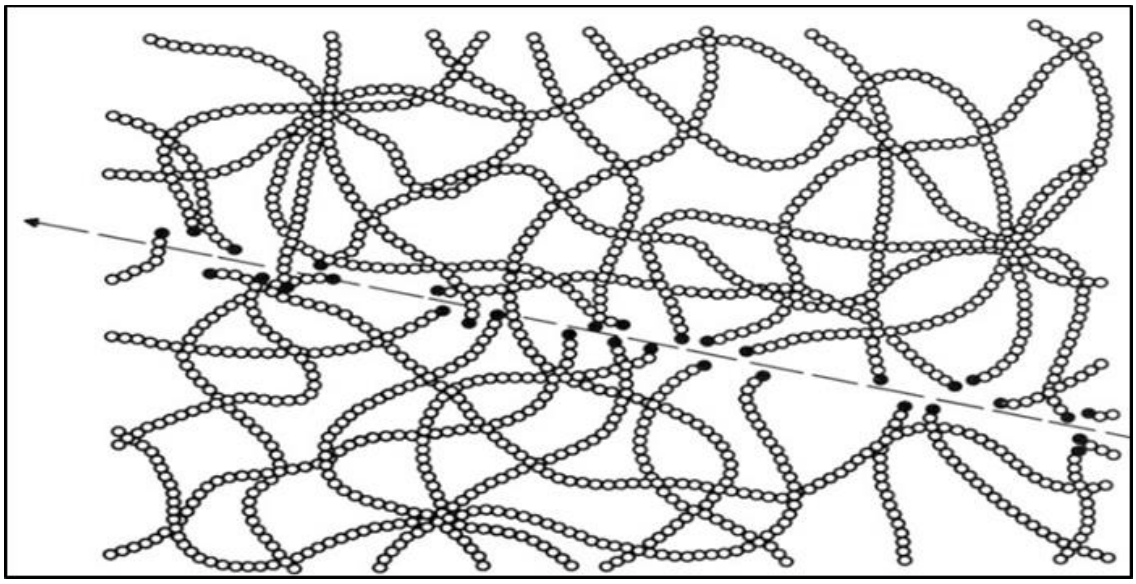

Figure 3. 4 Chain Breaking Mechanism in CR-39

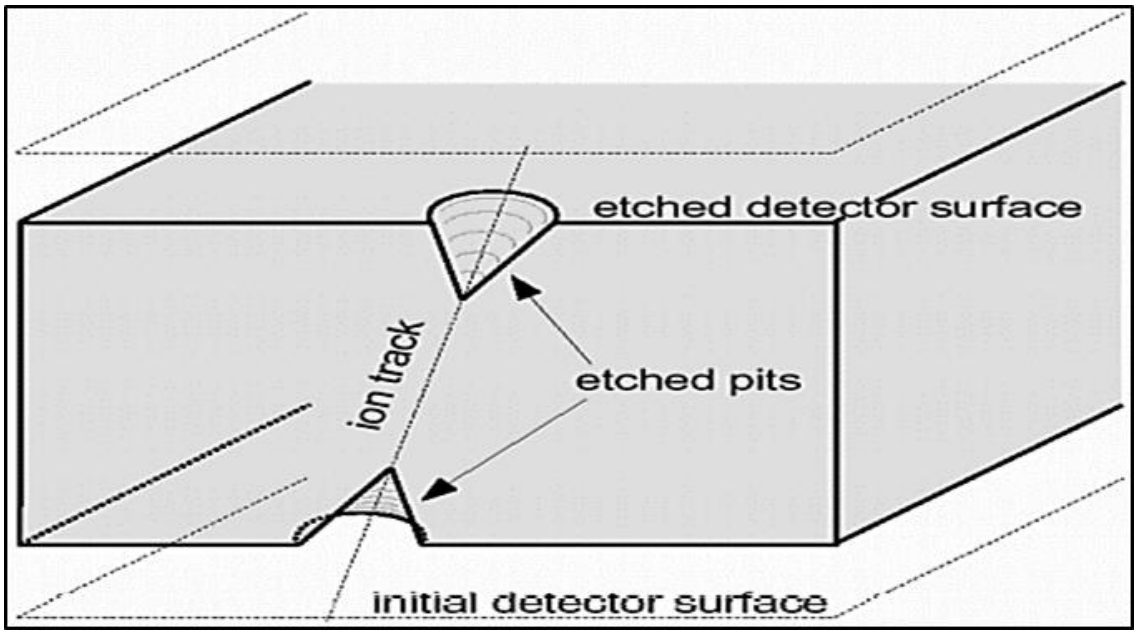

Figure 3. 5 The effect of the chemical etching process on the detector

Chapter Four

Methodology

Chapter Four

Methodology

4.1. The Study area

Tammoun is a Palestinian city in Tubas Governorate located in the northeast of the West Bank, at the confluence of latitude 32.28º north, and longitude 35.38º east. It is bordered to the north by Tubas city which is 5 km away, bordered to the south by Al aqrabaniah and Al-Nasaria, Wadi Al Far'a village and El Far'a Camp to the west and by Khirbet 'Atuf (Al beqah plains to Jordanian River) to the east as shown in figure 4.1.

Figure 4. 1 Tammoun location map

The soil formation in the surveyed region is dominated by terra rossas, pale rendzinas, brown rendzinas and grumusols, while the rocks were dolomite and dolomite limestone characterized by low number of radioactive nuclei.

4.2. Study aims

In general, the study aimed to determine the concentration of radon in Tammoun dwellings, the annual radiation dose absorbed due to radon and the risk of lung cancer. Therefore, ninety CR-39 detectors were distributed inside the dwellings in different and random regions of the town of Tammoun. Where detectors were placed in different rooms to study the effect of ventilation, as well as placed on different floors to study the effect of elevation on radon concentration. The following table (4.1) shows the distribution of detectors in rooms in different areas.

4.3. Preparation of dosimeters

The CR-39 detector sheet is cut into small parts, with ($1\ cm \times 1\ cm$) dimensions. The detector has two sides, one used only for measurement and the other can engrave code on it to distinguish it from other detectors.

The detector is fixed to the bottom of the conical plastic cup as in Figure (4.2) by blu-tac, and the mouth of the cup is covered with a single layer of cling film (Polyethylene foil), which allows the radon gas to pass, preventing dust and radon progeny from entering and reducing moisture (Abu-Samreh et al., 2016).

Table 4. 1 The distribution of detectors to rooms in different areas.

		Number of detectors				
Region name	**Region code**	**Bedroom**	**Guestroom**	**Kitchen**	**Store**	**Total**
The eastern region	**R1**	**7**	**7**	**8**	**1**	**23**
The northern region	**R2**	**6**	**6**	**6**	**3**	**21**
The central region	**R3**	**5**	**5**	**3**	**1**	**14**
The southern region	**R4**	**3**	**4**	**4**	**0**	**11**
The western region	**R5**	**7**	**6**	**7**	**1**	**21**
Total		**28**	**28**	**28**	**6**	**90**

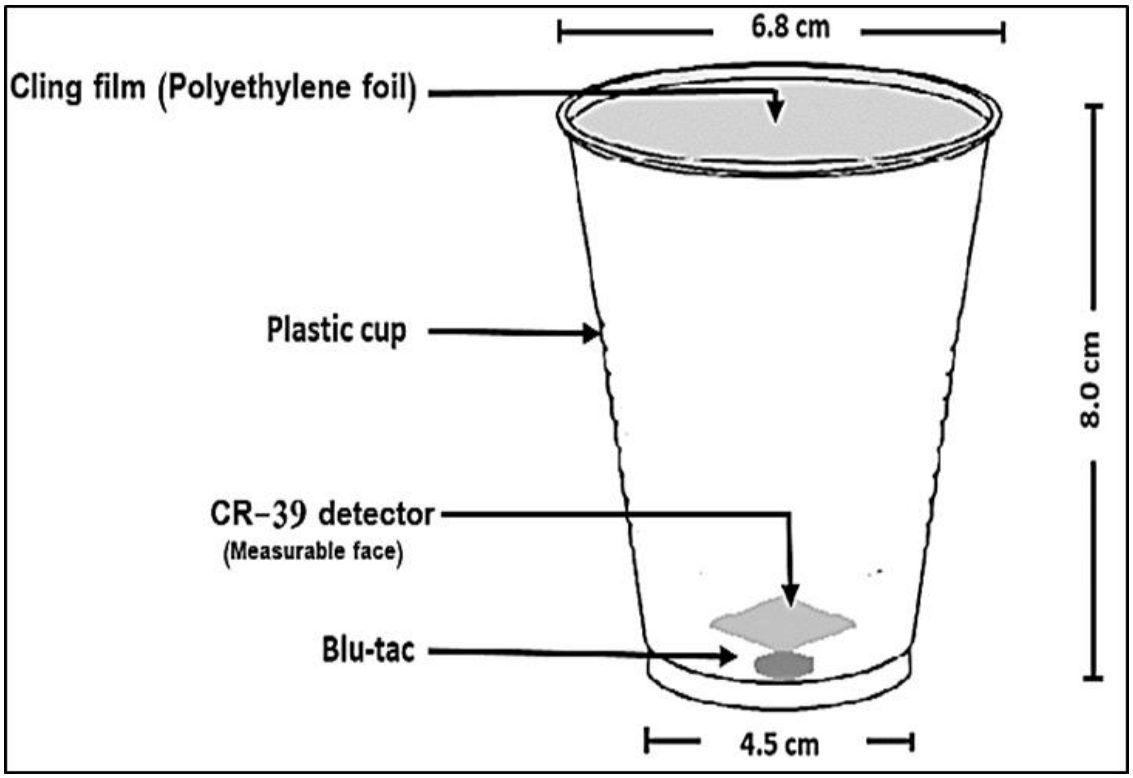

Figure 4. 2 Schematic diagram of the radon dosimeter

The prepared plastic cups are then hanged, which are called dosimeter, at a height of 1.5 meters from the ground and 10 cm from the side walls in the rooms for three months (Mallah et al., 2015).

4.4. Dosimeters collection

Dosimeters were distributed between September and December 2018, where each dosimeter remained for 90 days. The following table (4.2) shows the number of dosimeters distributed and collected, and the number of lost or damaged detectors.

Table 4. 2 Dosimeters distribution and collection in different regions of Tammoun town dwellings.

Region code	Distributions		Collection		number of days	Number of detectors		
	Date	Number of dosimeters	Date	Number of dosimeters		Lost	Damage	Measured
R1	7/9/2018	23	6/12/2018	22	90	1	1	21
R2	9/9/2018	21	8/12/2018	21	90	0	0	21
R3	11/9/2018	14	10/12/2018	14	90	0	0	14
R4	11/9/2018	11	10/12/2018	11	90	0	0	11
R5	9/9/2018	21	8/12/2018	18	90	3	1	17
Total	90		86			4	2	84

After collecting the dosimeters, the detectors were removed and stored in a small insulated box for transport to the laboratory.

4.5. Detectors etching

In the Chemistry Laboratory of An-Najah National University, a 6.25 N sodium hydroxide solution was prepared, adding 25 g of NaOH to 100 ml of distilled water. The experiment is prepared as shown in figure 4.3.

The detectors are then placed inside the flask. The solution is continuously stirred during the etching process using the Magnetic Stirring Bar which distributes NaOH evenly throughout the solution and prevents its accumulation.

Increasing the concentration of the solution due to evaporation can damage the reagents, so the condenser is used to keep the concentration stable.

The temperature is fixed at 75 ° C and monitored by the thermometer and the process lasts for 6 hours. After the end of the time period the concentration of the solution is reduced with distilled water to extract the reagents.

Then each detector is washed separately with distilled water and dried to move on to the scanning stage.

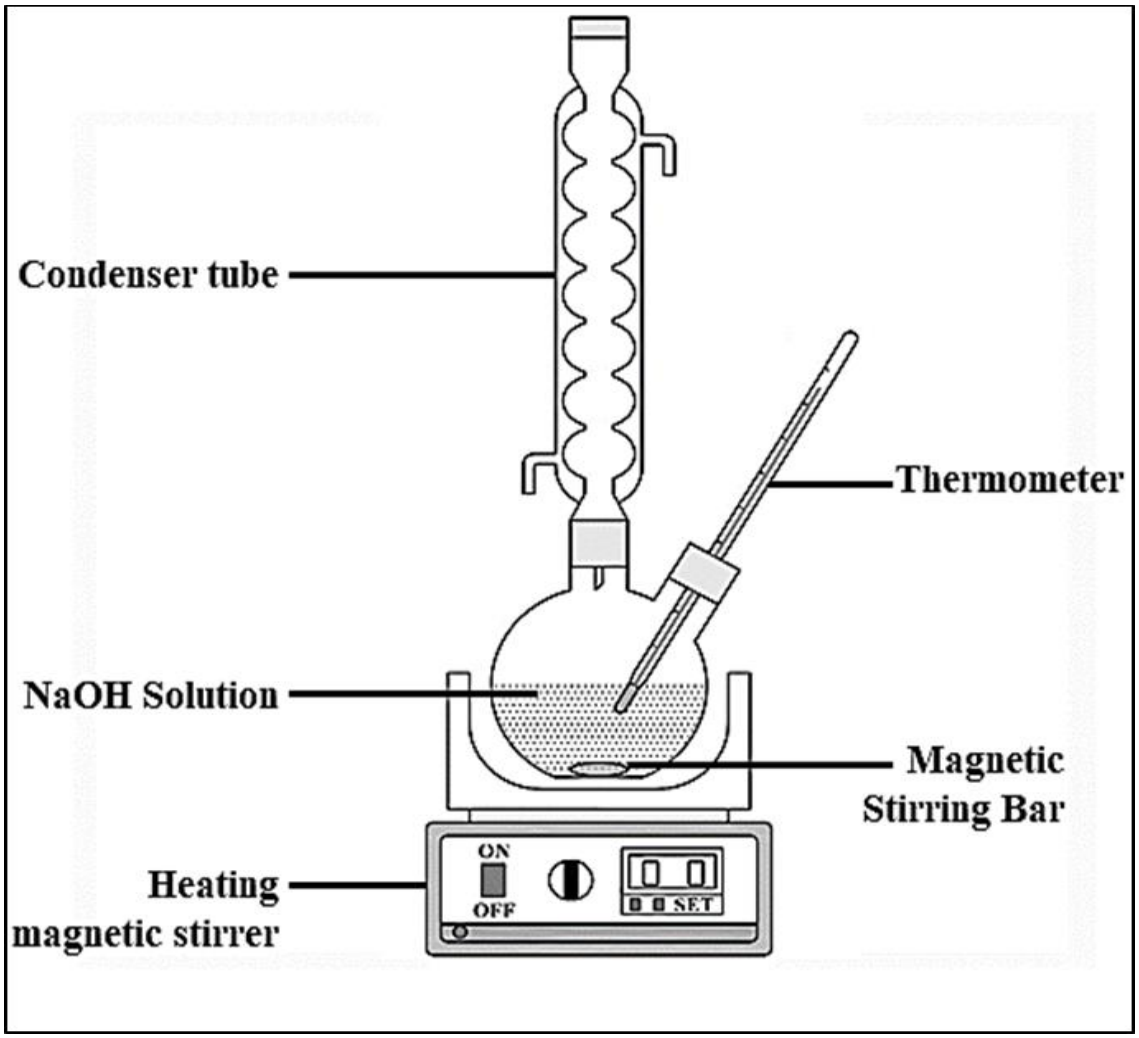

Figure 4. 3 Schematic diagram of experimental setup

4.6. Scanning process

The detectors were well cleaned to minimize dust and fingerprint effects. A digital optical microscope equipped with a camera with a magnification power of 400 is used to count the alpha tracks on the surface of detector. The detectors are well cleaned to minimize dust and fingerprint effects. Then the scanning process is carried out where the surface of the detector is divided into 15 circular fields, each with an area of

$53.1 \times 10^{-4} cm^2$, so after counting the number of alpha tracks in each field, the average number of tracks per cm^2 is calculated for each detector.

Figure (4.4) shows the alpha tracks as shown by the microscope

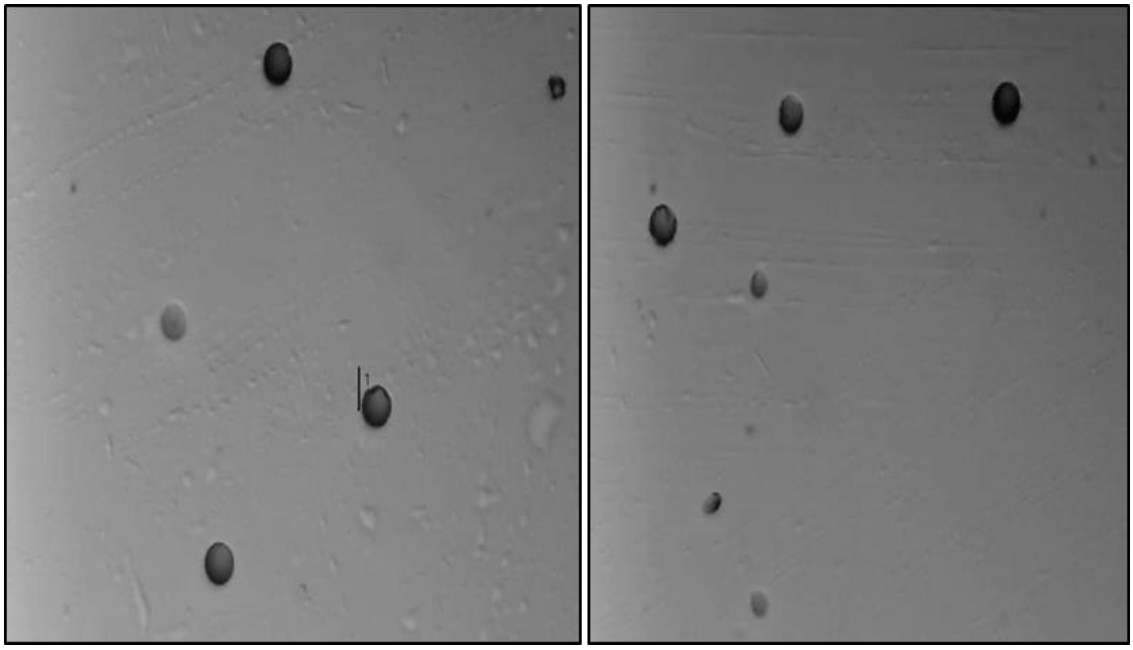

Figure 4. 4 Two images showing alpha tracks on the surface of the CR-39 detector

4.7. Indoor Radon measurements

4.7.1. Radon concentration:

The indoor radon concentration (C_{Rn}) can be calculated in (Bq/m^3) after finding the average number of tracks per detector in ($1cm^2$) and using the following equation (Khalef et al., 2016, Hashim et al., 2019):

$$C_{Rn} = \frac{\mathrm{k}\rho}{t} \qquad (4.1)$$

where:

$k = The\ calibration\ factor\ \left[5\ \frac{\left(\frac{Bq \cdot day}{m^3}\right)}{\left(\frac{\text{tracks}}{cm^2}\right)}\right]$ (Dwaikat et al., 2010)

ρ = The track density in $\left(\frac{\text{tracks}}{cm^2}\right)$

t = The time exposure (day)

4.7.2. The effective annual dose:

The calculation of the indoor radon concentration can be used to calculate the effective annual dose from radon exposure using the following formula (UNSCEAR 2000, F. Shoqwara 2012):

$$E = C_{Rn} \times H \times F \times D \times t \quad (4.2)$$

Where:

E = The annual effective dose ($\frac{mSv}{y}$)

F = The equilibrium factor (0.4)

H = The occupancy factor (0.8)

D = The dose conversion factor (9×10^{-6} $\frac{mSv}{\text{Bq.h.m}^{-3}}$)

t = The exposure time in year (8760 h).

4.7.3. Potential alpha energy concentration (PAEC)

(PAEC) can be estimated according to the following equation (Khalef et al., 2016):

$$PAEC(WL) = \frac{FC_{Rn}}{3700} \quad (4.3)$$

Work level (WL) is defined as the potential alpha energy concentration of 1.3×10^5 MeV/m^3 of air.

(PAEC) in terms of work level month (WLM) units is given by (Khalef et al., 2016):

$$PAEC(WLM) = 0.01 \times F \times C_{Rn}$$

and (WLM/y) can be calculated using the equation (Khalef et al., 2016):

$$PAEC(WLM/y) = PAEC(WL) * 40 \quad (4.4)$$

4.7.4. Lung cancer cases per year per million person

The absorption effective dose equivalent (AEDE) can be found using the equation (Khalef et al., 2016):

$$AEDE(mSv/y) = PAEC(WLM/y) * 5.5(mSv/WLM) \quad (4.5)$$

where $5.5(mSv/WLM)$ is the dose conversion factor.

There after, lung cancer cases per year per million person can be found using the equation (Khalef et al., 2016):

$$= AEDE(mSv/y) * 18 \times 10^{-6}(mSv)^{-1} \quad (4.6)$$

Chapter Five

Results

Chapter Five

Results

5.1. Introduction

In this chapter, the results of radon measurements are presented. Six of these detectors (6.67%) were damaged or lost, and the rest of the results were analyzed in detail as shown in (Appendix A).

Also in this chapter, the effect of three main factors on the obtained results i.e. geographic location, floor level and room type, were analyzed.

5.2. Results of radon measurements in Tammoun town

The following tables show the results of radon measurements for Tammoun town in five tables (from Table 5.1 to Table 5.5). Each table contains results of indoor radon concentration, effective annual dose, potential alpha energy concentration and lung cancer cases per year per million persons in one region.

The abbreviation (X) in the Room Type column indicates the bedroom, kitchen (Y), guestroom (Z), and store (W).

The abbreviation (GF) in the floor level column refers to the ground floor and (F1) to the first floor. The error in the following tables is the standard mean error (SE) and standard deviation (SD) which can be found using the following formula:

$$SE = \frac{SD}{\sqrt{N}} \tag{5.1}$$

$$SD = \sqrt{\frac{\sum(value - mean)^2}{N}} \tag{5.2}$$

where N is the number of value in the data set.

Table (5.1): Indoor radon concentrations, effective annual dose, potential alpha energy concentration and lung cancer cases per year per million person of the southern region (R4).

Sample No. / Serial No.	Dosimeter Sample No.	Room Type	Floor Level	$C_{Rn}(Bq/m^3) \pm$ SE			effective annual dose (mSv/y)	PAEC (WLM/y)	(Lung Cancer Cases per Year per Million Person) $\times 10^{-5}$
1	124	Y	GF	31.45	±	0.26	0.79	0.14	1.35
2	121	X	GF	30.75	±	0.23	0.78	0.13	1.32
3	104	Y	F1	16.07	±	0.17	0.41	0.07	0.69
4	43	X	F1	40.53	±	0.35	1.02	0.18	1.74
5	88	Z	F1	30.05	±	0.29	0.76	0.13	1.29
6	120	Y	GF	26.55	±	0.29	0.67	0.11	1.14
7	102	Z	GF	46.12	±	0.34	1.16	0.20	1.97
8	123	Z	GF	34.24	±	0.25	0.86	0.15	1.47
9	110	Z	GF	30.05	±	0.19	0.76	0.13	1.29
10	93	X	GF	34.94	±	0.23	0.88	0.15	1.50
11	122	Y	GF	35.64	±	0.24	0.90	0.15	1.53
Avg. Radon Concentration ± SE = $(32.40 \pm 2.32)\ Bq/m^3$									
Avg. Effective annual dose ± SE = (0.82 ± 0.06) mSv/y									
Avg. Lung Cancer Cases per Year per Million Person ± SE = $(1.39 \pm 0.10) \times 10^{-5}$									

Table (5.2): Indoor radon concentrations, effective annual dose, potential alpha energy concentration and lung cancer cases per year per million person of the eastern region (R1).

Serial No.	Dosimeter Sample No.	Room Type	Floor Level	$C_{Rn}(Bq/m^3) \pm SE$			effective annual dose (mSv/y)	PAEC (WLM/y)	(Lung Cancer Cases per Year per Million Person) $\times 10^{-5}$
1	55	X	F1	34.24	±	0.21	0.86	0.15	1.47
2	44	Z	F1	38.43	±	0.27	0.97	0.17	1.65
3	22	Y	F1	25.16	±	0.19	0.63	0.11	1.08
4	26	Y	GF	18.17	±	0.18	0.46	0.08	0.78
5	58	Z	GF	28.65	±	0.21	0.72	0.12	1.23
6	36	X	GF	26.55	±	0.24	0.67	0.11	1.14
7	20	Y	GF	27.25	±	0.21	0.69	0.12	1.17
8	15	Z	GF	35.64	±	0.32	0.90	0.15	1.53
9	34	X	GF	24.46	±	0.16	0.62	0.11	1.05
10	21	Z	GF	27.95	±	0.16	0.71	0.12	1.20
11	78	X	GF	24.46	±	0.13	0.62	0.11	1.05
12	54	X	F1	27.95	±	0.19	0.71	0.12	1.20
13	91	Z	F1	22.36	±	0.13	0.56	0.10	0.96
14	8	Y	F1	27.95	±	0.25	0.71	0.12	1.20
15	73	Y	GF	34.24	±	0.23	0.86	0.15	1.47
16	97	Z	GF	34.94	±	0.23	0.88	0.15	1.50
17	13	X	GF	28.65	±	0.18	0.72	0.12	1.23
18	23	Z	F1	37.04	±	0.27	0.93	0.16	1.59
19	95	Y	F1	25.86	±	0.24	0.65	0.11	1.11
20	41	X	F1	36.34	±	0.39	0.92	0.16	1.56
21	82	Y	GF	22.36	±	0.26	0.56	0.10	0.96
Avg. Radon Concentration ± SE = $(28.98 \pm 1.22)\ Bq/m^3$									
Avg. Effective annual dose ± SE = (0.73 ± 0.03) mSv/y									
Avg. Lung Cancer Cases per Year per Million Person ± SE = $(1.24 \pm 0.05) \times 10^{-5}$									

Table (5.3): Indoor radon concentrations, effective annual dose, potential alpha energy concentration and lung cancer cases per year per million person of the northern region (R2).

Serial No.	Dosimeter Sample No.	Room Type	Floor Level	$C_{Rn}(Bq/m^3) \pm$ SE			effective annual dose	PAEC (WLM/y)	(Lung Cancer Cases per Year per Million Person)
1	7	Z	GF	27.25	±	0.31	0.69	0.12	1.17
2	29	Y	GF	21.66	±	0.18	0.55	0.09	0.93
3	89	X	GF	27.25	±	0.29	0.69	0.12	1.17
4	74	Z	F1	23.06	±	0.11	0.58	0.10	0.99
5	31	Y	F1	34.24	±	0.28	0.86	0.15	1.47
6	75	X	F1	22.36	±	0.13	0.56	0.10	0.96
7	69	Z	F1	25.86	±	0.22	0.65	0.11	1.11
8	6	Y	F1	20.27	±	0.18	0.51	0.09	0.87
9	90	X	F1	24.46	±	0.16	0.62	0.11	1.05
10	96	W	GF	29.35	±	0.20	0.74	0.13	1.26
11	16	W	GF	31.45	±	0.24	0.79	0.14	1.35
12	57	Y	F1	34.24	±	0.40	0.86	0.15	1.47
13	40	Z	F1	31.45	±	0.29	0.79	0.14	1.35
14	99	X	F1	25.16	±	0.16	0.63	0.11	1.08
15	56	Z	GF	30.05	±	0.24	0.76	0.13	1.29
16	98	Y	GF	25.16	±	0.16	0.63	0.11	1.08
17	83	X	GF	30.75	±	0.28	0.78	0.13	1.32
18	71	Y	GF	56.60	±	0.54	1.43	0.24	2.42
19	72	X	GF	33.54	±	0.28	0.85	0.15	1.44
20	87	Z	GF	30.75	±	0.21	0.78	0.13	1.32
21	100	W	GF	34.24	±	0.30	0.86	0.15	1.47
Avg. Radon Concentration ± SE = $(29.48 \pm 1.66)\ Bq/m^3$									
Avg. Effective annual dose ± SE = (0.74 ± 0.04) mSv/y									
Avg. Lung Cancer Cases per Year per Million Person ± SE = $(1.26 \pm 0.07) \times 10^{-5}$									

Table (5.4): Indoor radon concentrations, effective annual dose, potential alpha energy concentration and lung cancer cases per year per million person of the central region (R3).

Serial No.	Dosimeter Sample No.	Room Type	Floor Level	$C_{Rn}(Bq/m^3) \pm$ SE			effective annual dose (mSv/y)	PAEC (WLM/y)	(Lung Cancer Cases per Year per Million Person) $\times 10^{-5}$
1	38	Z	F1	24.46	±	0.13	0.62	0.11	1.05
2	101	Y	F1	53.81	±	0.19	1.36	0.23	2.30
3	112	X	F1	27.25	±	0.21	0.69	0.12	1.17
4	1	X	F1	25.16	±	0.16	0.63	0.11	1.08
5	14	X	GF	24.46	±	0.13	0.62	0.11	1.05
6	25	Y	GF	28.65	±	0.23	0.72	0.12	1.23
7	76	Z	GF	22.36	±	0.13	0.56	0.10	0.96
8	108	Z	F1	30.75	±	0.32	0.78	0.13	1.32
9	106	W	GF	30.75	±	0.23	0.78	0.13	1.32
10	107	X	GF	28.65	±	0.15	0.72	0.12	1.23
11	105	Y	GF	25.86	±	0.22	0.65	0.11	1.11
12	28	X	F1	25.86	±	0.19	0.65	0.11	1.11
13	92	Z	F1	23.76	±	0.18	0.60	0.10	1.02
14	59	Z	GF	26.55	±	0.26	0.67	0.11	1.14
Avg. Radon Concentration ± SE = $(28.45 \pm 2.06)\ Bq/m^3$									
Avg. Effective annual dose ± SE = **(0.72 ± 0.05) mSv/y**									
Avg. Lung Cancer Cases per Year per Million Person ± SE = $(1.22 \pm 0.88) \times 10^{-5}$									

Table (5.5): Indoor radon concentrations, effective annual dose, potential alpha energy concentration and lung cancer cases per year per million person of the western region (R5).

Serial No.	Dosimeter Sample No.	Room Type	Floor Level	$C_{Rn}(Bq/m^3) \pm$ SE			effective annual dose (mSv/y)	PAEC (WLM/y)	(Lung Cancer Cases per Year per Million Person) $\times 10^{-5}$
1	12	Y	F1	29.35	±	0.22	0.74	0.13	1.26
2	39	Z	F1	37.04	±	0.22	0.93	0.16	1.59
3	81	X	F1	30.05	±	0.31	0.76	0.13	1.29
4	32	Z	GF	21.66	±	0.21	0.55	0.09	0.93
5	42	X	GF	34.24	±	0.23	0.86	0.15	1.47
6	46	Y	GF	25.86	±	0.22	0.65	0.11	1.11
7	35	X	GF	27.25	±	0.16	0.69	0.12	1.17
8	45	Y	GF	24.46	±	0.19	0.62	0.11	1.05
9	77	Z	F1	24.46	±	0.19	0.62	0.11	1.05
10	86	Y	F1	20.96	±	0.14	0.53	0.09	0.90
11	51	X	F1	33.54	±	0.28	0.85	0.15	1.44
12	24	Y	GF	28.65	±	0.15	0.72	0.12	1.23
13	52	Z	GF	27.25	±	0.27	0.69	0.12	1.17
14	17	X	GF	30.05	±	0.35	0.76	0.13	1.29
15	70	Y	F1	27.25	±	0.25	0.69	0.12	1.17
16	30	Z	F1	22.36	±	0.17	0.56	0.10	0.96
17	79	X	F1	25.16	±	0.16	0.63	0.11	1.08
Avg. Radon Concentration ± SE = $(27.62 \pm 1.09)\ Bq/m^3$									
Avg. Effective annual dose ± SE = (0.70 ± 0.03) mSv/y									
Avg. Lung Cancer Cases per Year per Million Person ± SE = $(1.18 \pm 0.05) \times 10^{-5}$									

The distribution of the indoor radon concentration in Tammoun town is shown in Figure 5.1 varied from a minimum of 16.07 ± 0.07 to a maximum of 56.60 ± 0.54 with mean of 28.98 ± 1.22 Bq/m^3 (Table 5.6).

Table (5.6): The minimum, maximum, mean, standard deviation and standard error of the mean value of radon concentrations in Tammoun town.

Min	Max	Mean	SD	SE
16.07	56.60	29.19	6.61	0.72

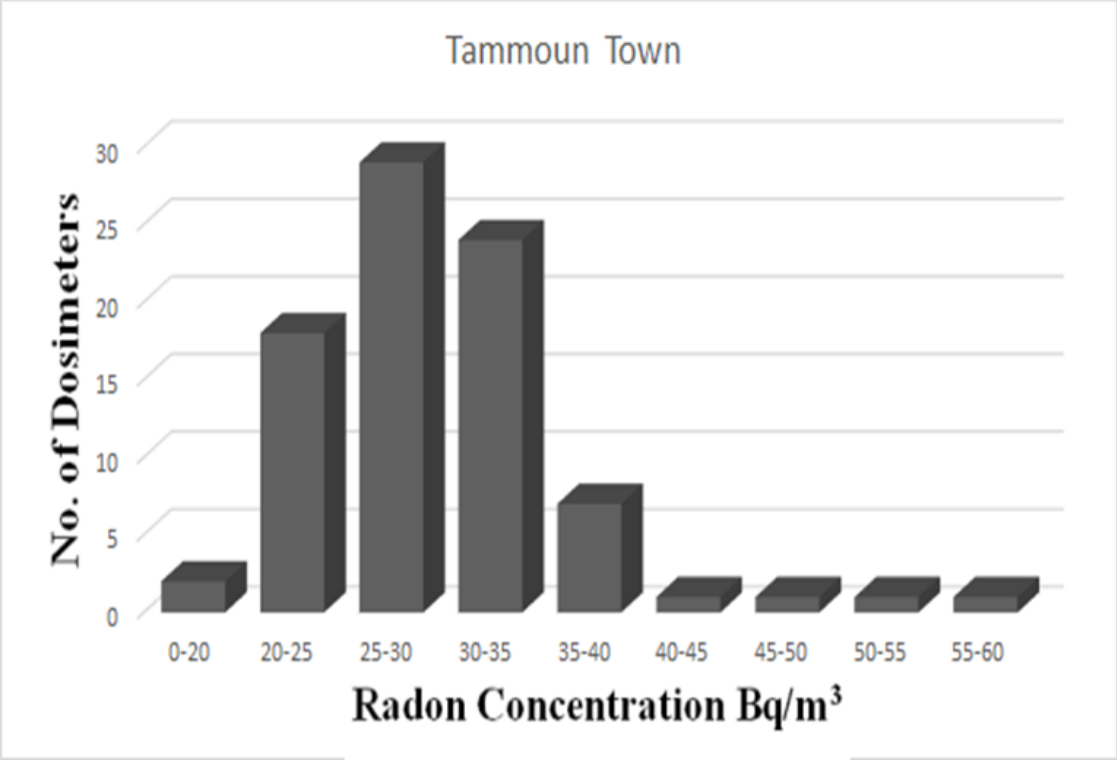

Figure 5. 1 Radon concentration distribution in Tammoun town.

The effective annual dose for dwellers in Tammoun town was varied from 0.4 to 1.43 with mean of 0.74 ± 0.02 mSv/y.

The lung cancer cases per year per million persons for dwellers in Tammoun town was worked out to be about (1.25± 0.03) × 10^{-5}.

5.2.1. Geographic location effect with radon concentration

The town was divided into five areas to study the impact of geographical location on radon concentration: the eastern region, the northern region, the central region, the southern region and the western region.

The average radon concentrations for each region were respectively: 28.98 ± 1.22 Bq/m^3, 29.48 ± 1.66 Bq/m^3, 28.45 ± 2.06 Bq/m^3, 32.40 ± 2.32 Bq/m^3 and 27.62 ± 1.09 Bq/m^3. The minimum concentrations were 18.17 Bq/m^3, 20.27 Bq/m^3, 22.36 Bq/m^3, 16.07 Bq/m^3 and 20.96 Bq/m^3 and the maximum concentrations were: 38.43 Bq/m^3, 56.60 Bq/m^3, 53.81 Bq/m^3, 46.12 Bq/m^3 and 37.04 Bq/m^3 (as shown in Table 5.7) and (Figure 5.2)

Table (5.7): The minimum, maximum, mean, standard deviation and standard error of the mean value of radon concentrations in the five regions.

Region	Min	Max	Mean	SD	SE
R1	18.17	38.43	28.98	5.59	1.22
R2	20.27	56.60	29.48	7.60	1.66
R3	22.36	53.81	28.45	7.72	2.06
R4	16.07	46.12	32.40	7.68	2.32
R5	20.96	37.04	27.62	4.48	1.09

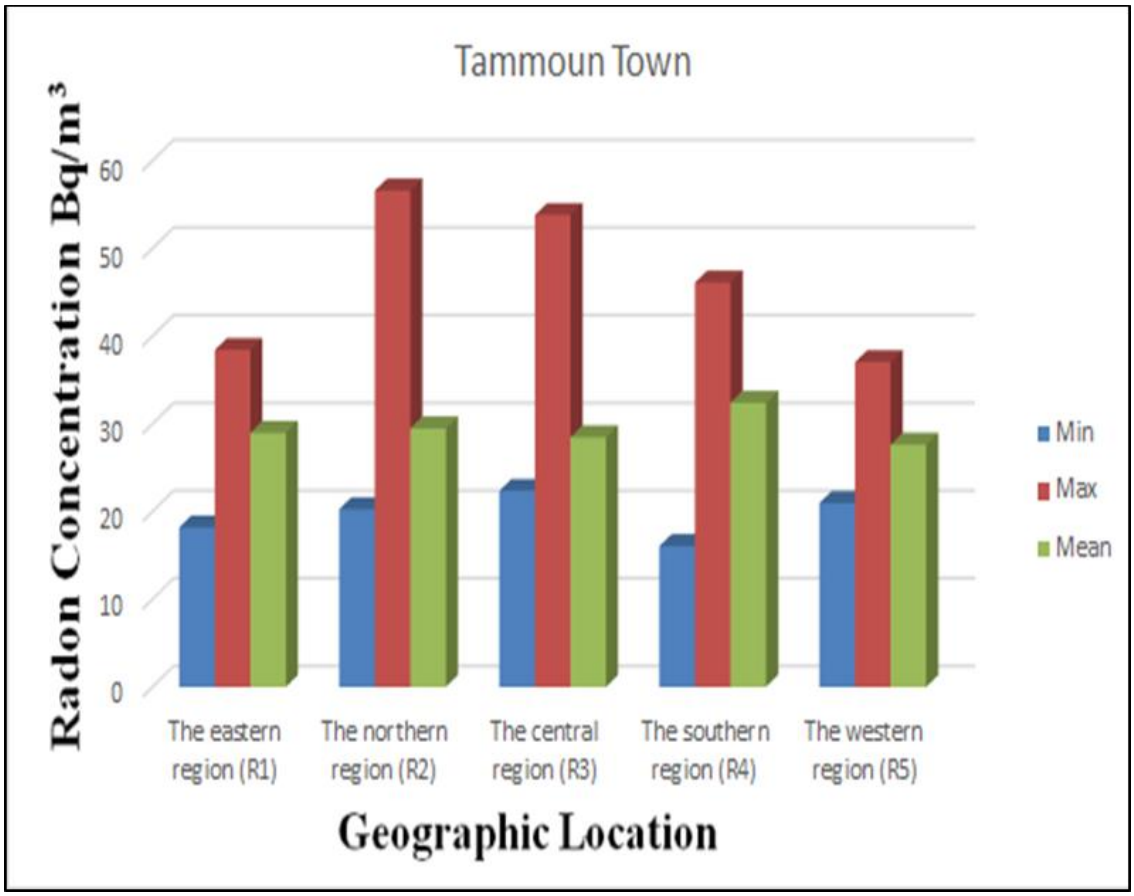

Figure 5. 2 The average radon concentration in the five regions.

The effective annual dose was found to be 0.73 ± 0.03 mSv/y in the eastern region, 0.74 ± 0.04 mSv/y in the northern region, 0.72 ± 0.05 mSv/y in the central region, 0.82 ± 0.06 mSv/y in the southern region and 0.70 ± 0.03 mSv/y in the western region (as shown in Table 5.8).

The lung cancer cases per year per million person was found to be (1.24± 0.05) $\times 10^{-5}$ in the eastern region, (1.26± 0.07) $\times 10^{-5}$ in the northern region, (1.22± 0.09) $\times 10^{-5}$ in the central region, (1.39 ± 0.10) $\times 10^{-5}$ in the southern region and (1.18± 0.05) $\times 10^{-5}$ in the western region (as shown in Table 5.8).

Table (5.8): Summary analysis of the average radon concentrations, effective annual dose and lung cancer cases per year per million person in the five regions.

Region name	Number of dosimeters	$C_{Rn}(Bq/m^3) \pm SE$	effective annual dose (mSv/y)	(Lung Cancer Cases per Year per Million Person) $\times 10^{-5}$
The eastern region (R1)	21	28.98 ± 1.22	0.73 ± 0.03	1.24 ± 0.05
The northern region (R2)	21	29.48 ± 1.66	0.74 ± 0.04	1.26 ± 0.07
The central region (R3)	14	28.45 ± 2.06	0.72 ± 0.05	1.22 ± 0.09
The southern region (R4)	11	32.04 ± 2.32	0.82 ± 0.06	1.39 ± 0.10
The western region (R5)	17	27.62 ± 1.09	0.70 ± 0.03	1.18 ± 0.05

Figure 5.3 and figure 5.4 show the distribution of radon concentration in the Western Region (R5) and the Eastern Region (R1) for 17 and 21 detectors, respectively.

Figure 5.5 and figure 5.6 represent the radon concentration in Central region (R3) and Northern region (R2).

Figure 5.7 represents the radon concentration in southern region (R4).

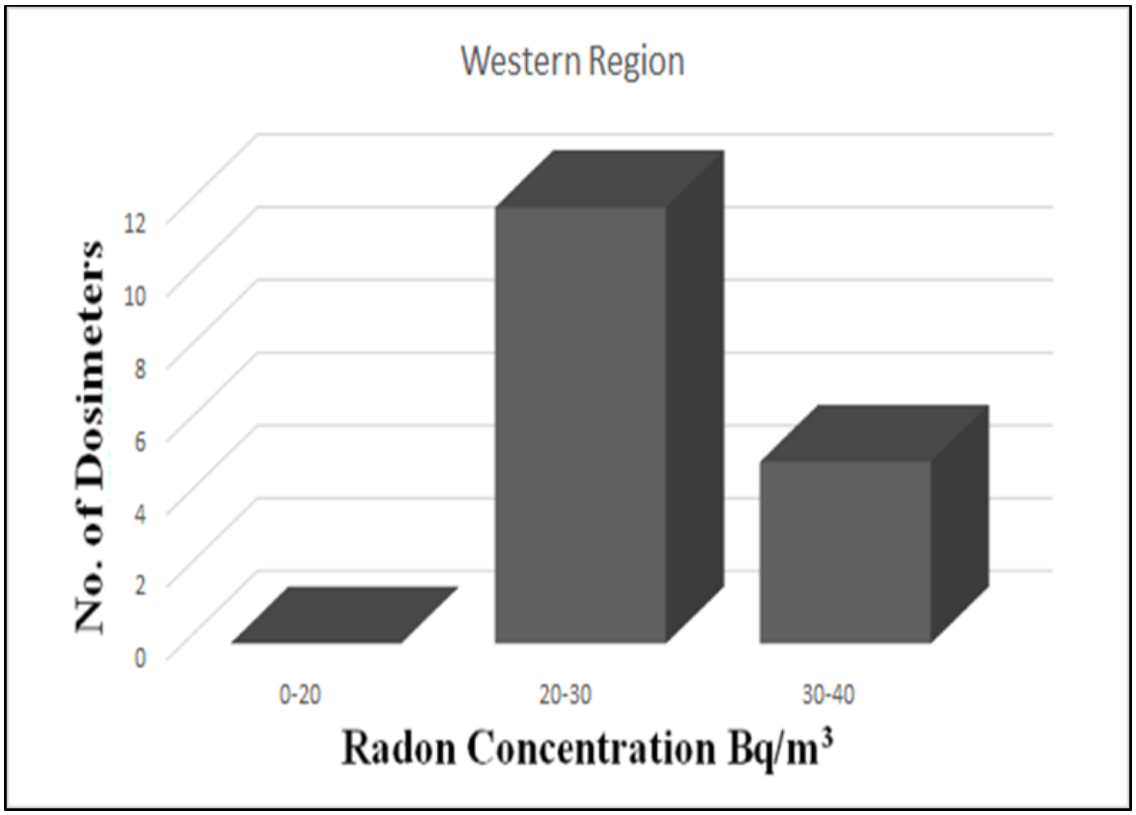

Figure 5. 3 Radon concentration distribution in Western Region (R5)

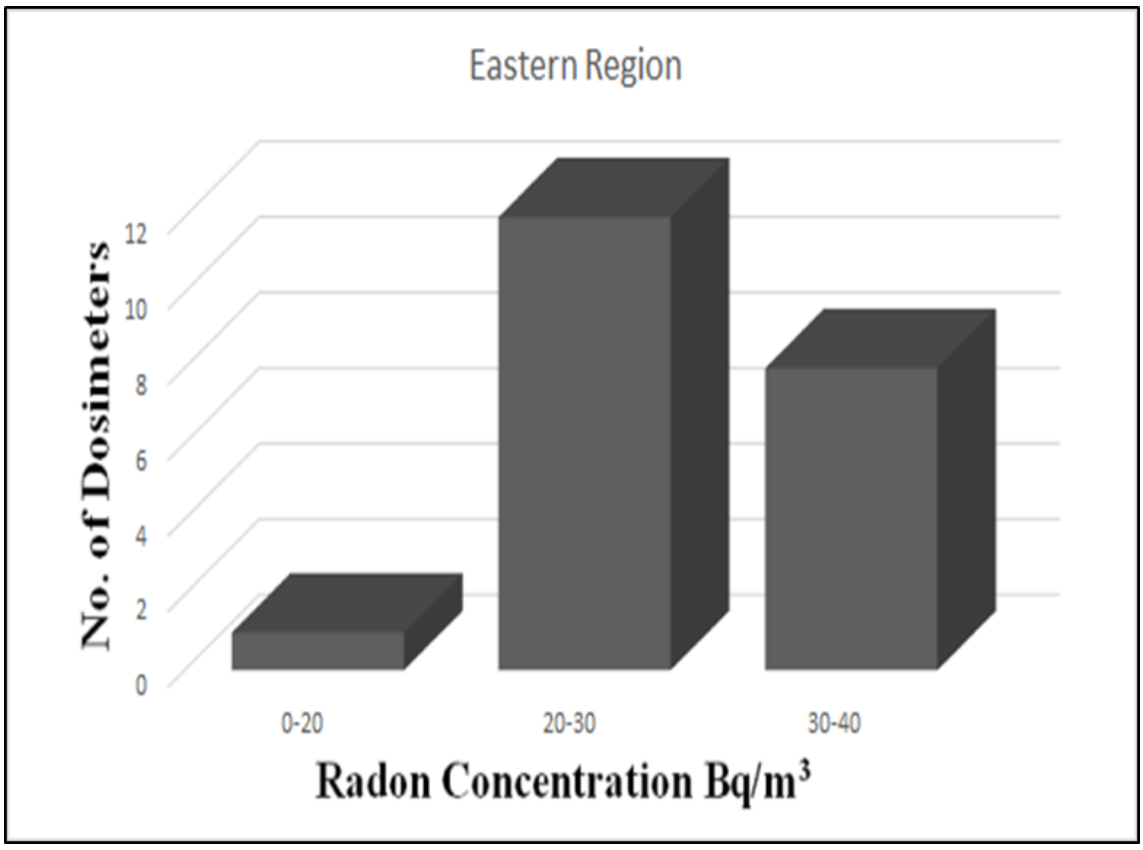

Figure 5. 4 Radon concentration distribution in Eastern Region (R1)

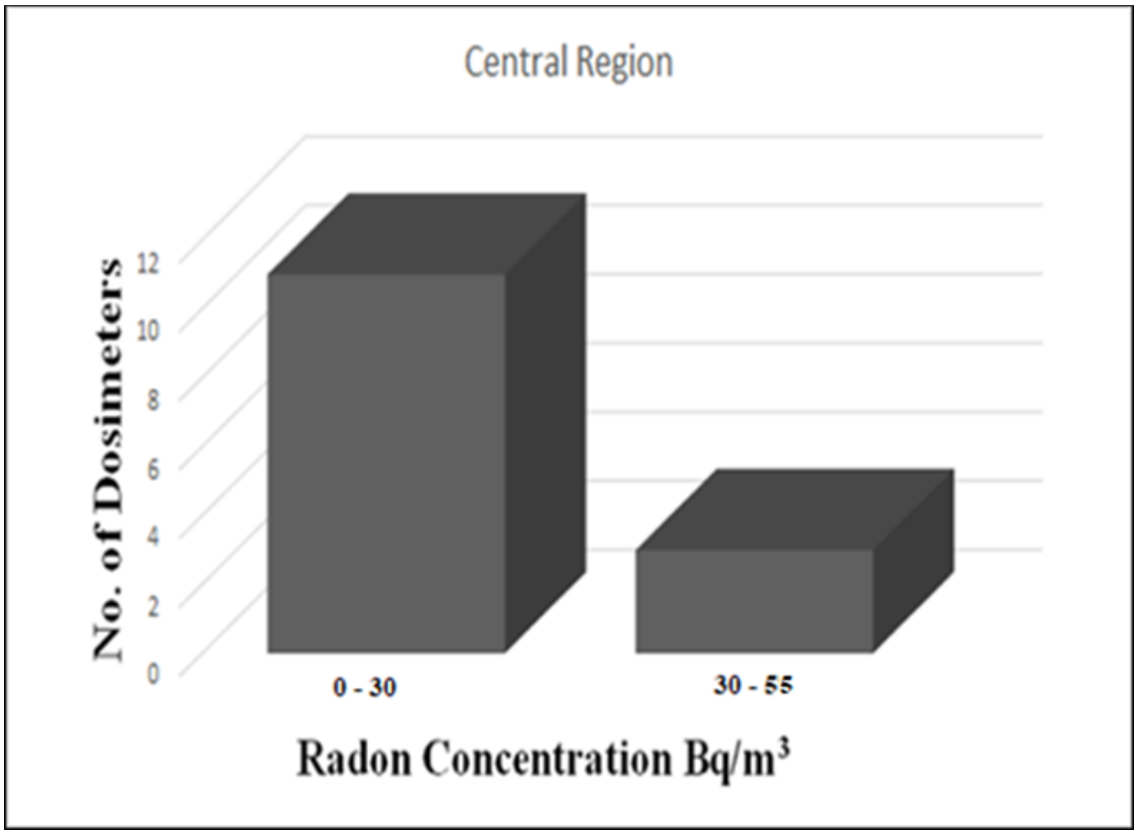

Figure 5. 5 Radon concentration distribution in Central Region (R3)

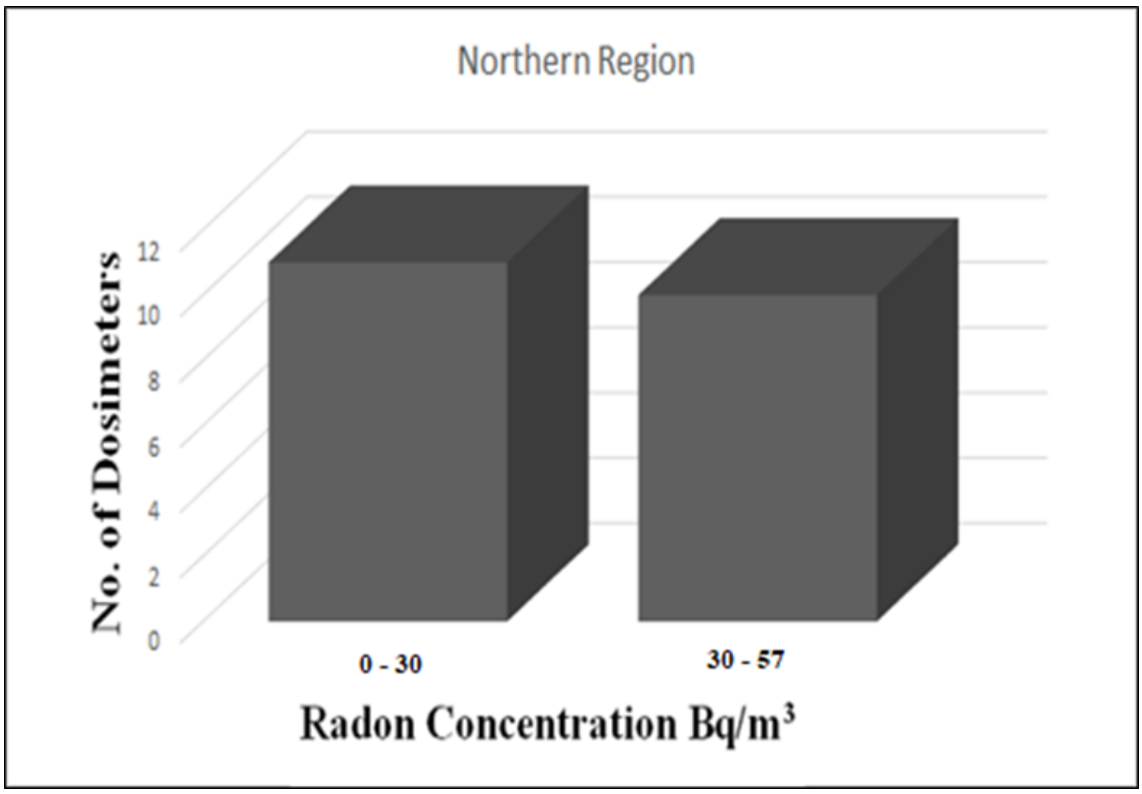

Figure 5. 6 Radon concentration distribution in Northern Region (R2).

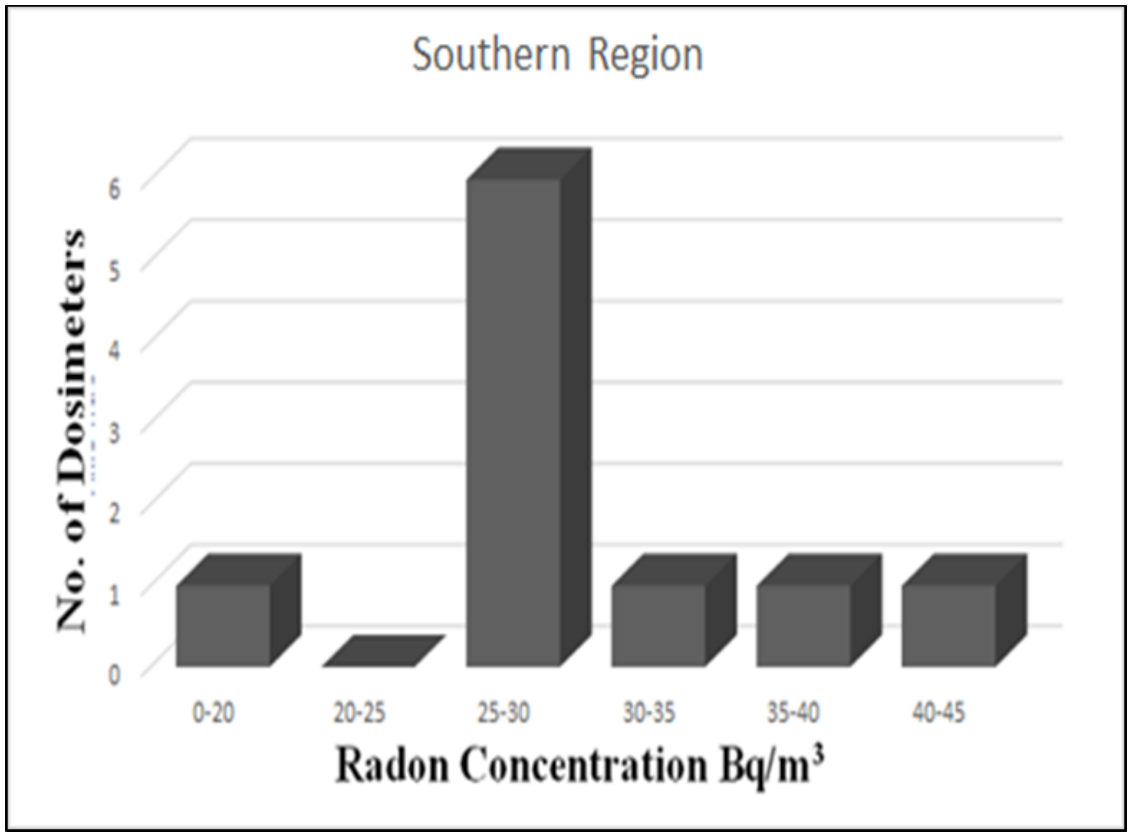

Figure 5. 7 Radon concentration distribution in Southern Region

5.2.2. Level floor effect with radon concentration

One of the factors affecting radon concentration is the height of the building above the ground. So the effect of the level of floors on radon concentration in ground floor (GF) and first floor (F1) was investigated.

Average radon concentrations for ground and first floor respectively: 29.53 ± 0.92 Bq / m^3 and 28.76 ± 1.16 Bq / m^3 as shown in (Figure 5.8).

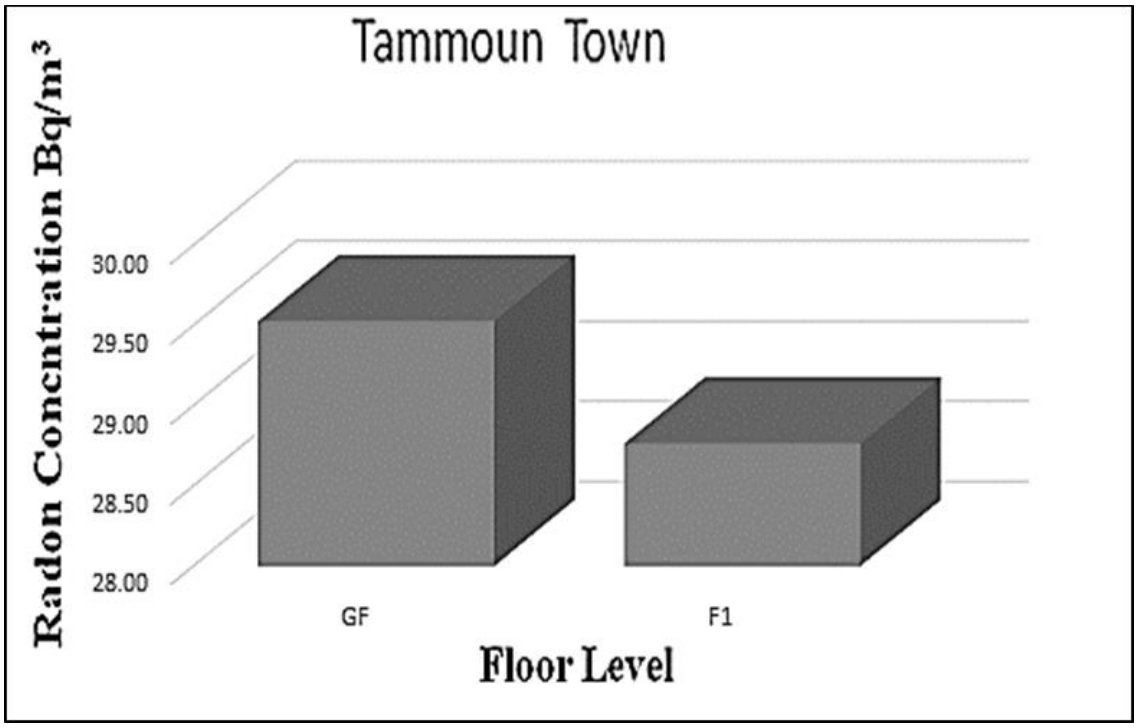

Figure 5. 8 The average radon concentration in the two levels

The lowest concentrations were 18.17 ± 0.18 Bq / m^3 and 16.07 ± 0.07 Bq / m^3, also the maximum concentrations are: 56.60 ± 0.54 Bq / m^3 and 53.81 ± 0.19 Bq / m^3 as shown in (Table 5.9).

Table (5.9): The minimum, maximum, mean, standard deviation and standard error of the mean value of radon concentrations in the two levels.

Floor level	Min	Max	Mean	SD	SE
GF	18.17	56.60	29.53	6.30	0.92
F1	16.07	53.81	28.76	7.06	1.16

Figure 5.9 and figure 5.10 represent the radon concentration distribution in ground floor (GF) and first floor (F1).

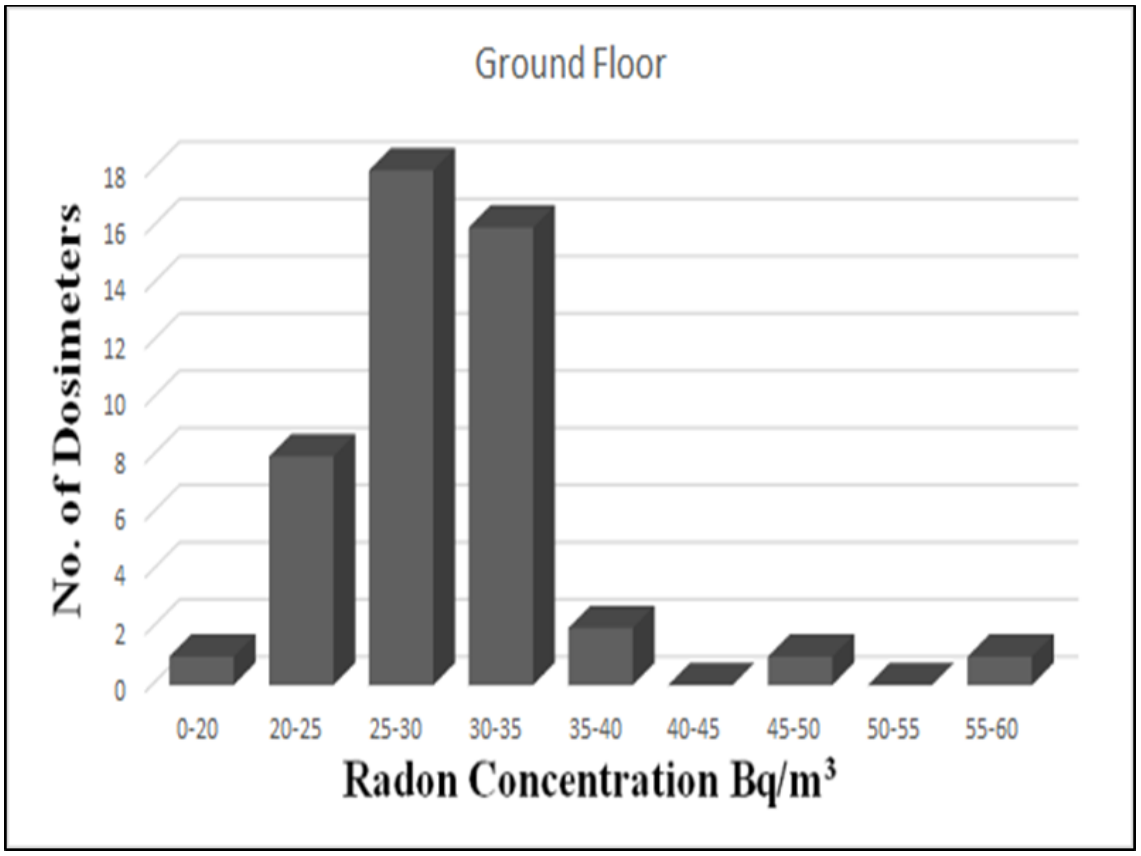

Figure 5. 9 Radon concentration distribution in ground floor.

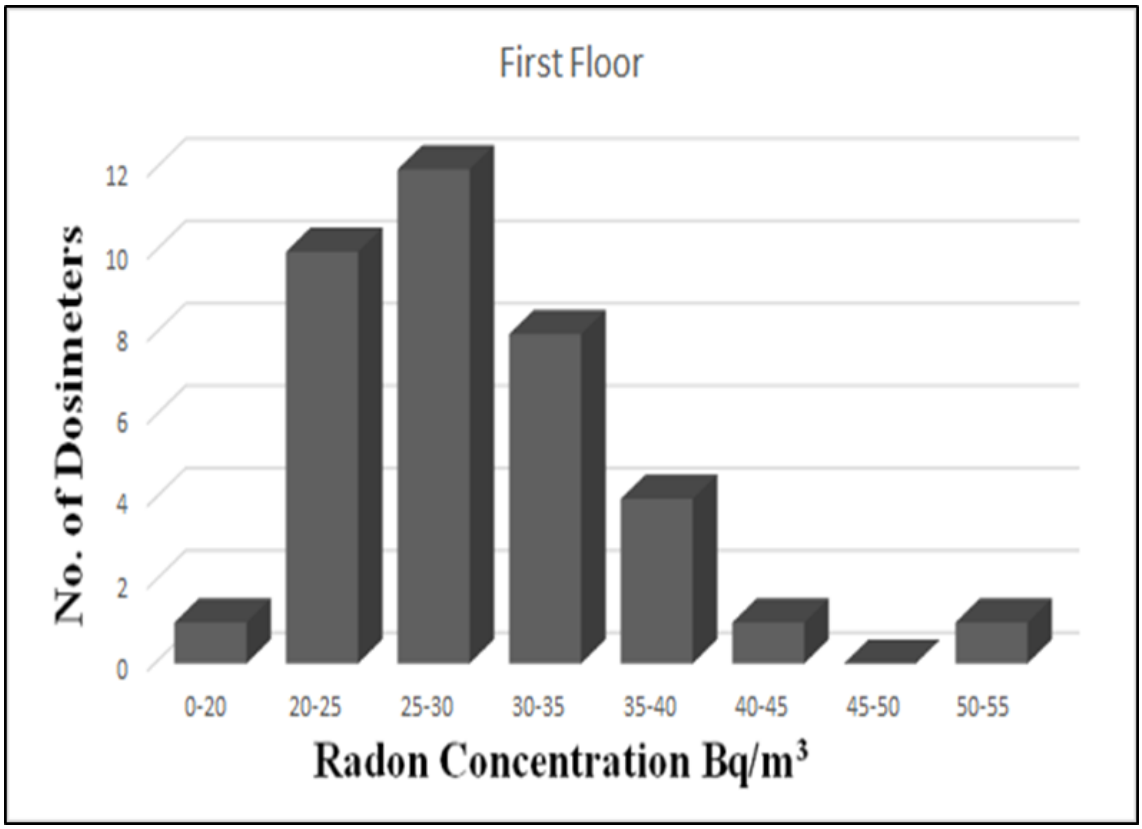

Figure 5. 10 Radon concentration distribution in first floor

5.2.3. Rooms type effect with radon concentration

Average radon concentrations for bedroom, living room, kitchen and store are respectively, 29.04 ± 0.86 Bq / m^3, 29.43 ± 1.16 Bq / m^3, 28.76 ± 1.81 Bq / m^3 and 31.45 ± 1.03 Bq / m^3.

The lowest concentrations were 22.36 ± 0.13 Bq / m^3, 21.66 ± 0.18 Bq / m^3, 16.07 ± 0.17 Bq / m^3 and 29.35 ± 0.22 Bq / m^3, while the maximum concentrations are: 40.53 ± 0.35 Bq / m^3, 46.12 ± 0.34 Bq / m^3, 56.60 ± 0.54 Bq / m^3 and 34.24 ± 0.30 Bq / m^3 as shown in (Table 5.10) and (Figure 5.11).

Table (5.10): The minimum, maximum, mean, standard deviation and standard error of the mean value of radon concentrations in the four type rooms.

Rooms type	Min	Max	Mean	SD	SE
bedroom	22.36	40.53	29.04	4.49	0.86
Guestrooms	21.66	46.12	29.43	6.02	1.16
kitchen	16.07	56.60	28.76	9.22	1.81
store	29.35	34.24	31.45	2.06	1.03

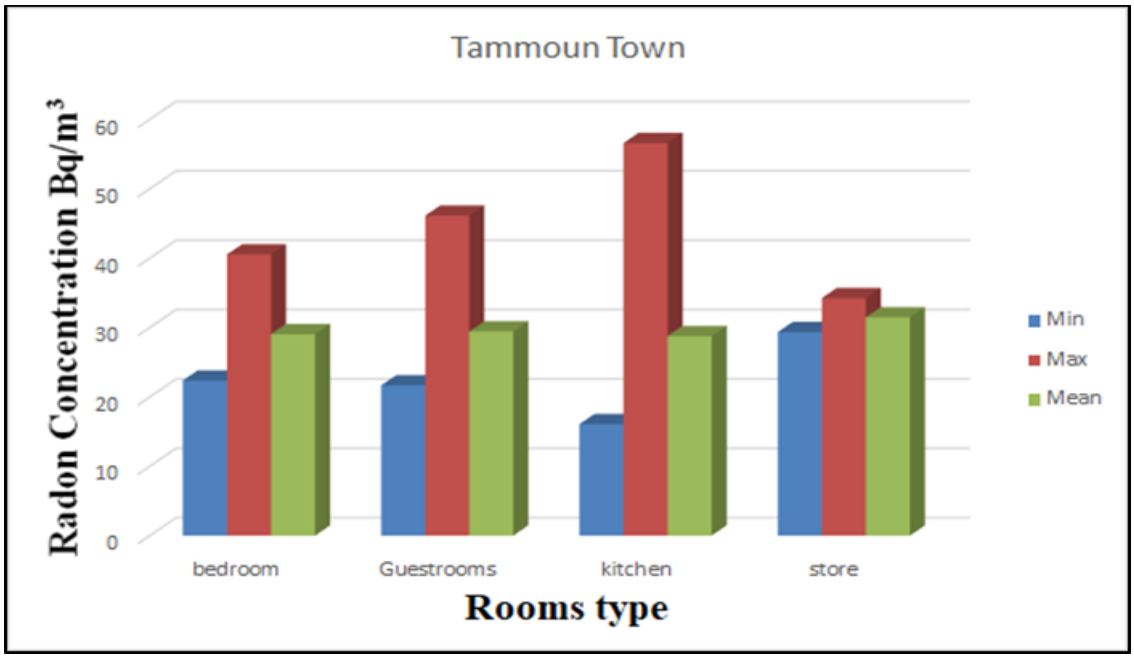

Figure 5. 11 Radon concentration distribution in the four type rooms.

Figures (5.12), (5.13) and (5.14) represent the radon concentration distribution in bedrooms, kitchens and Guestrooms respectively.

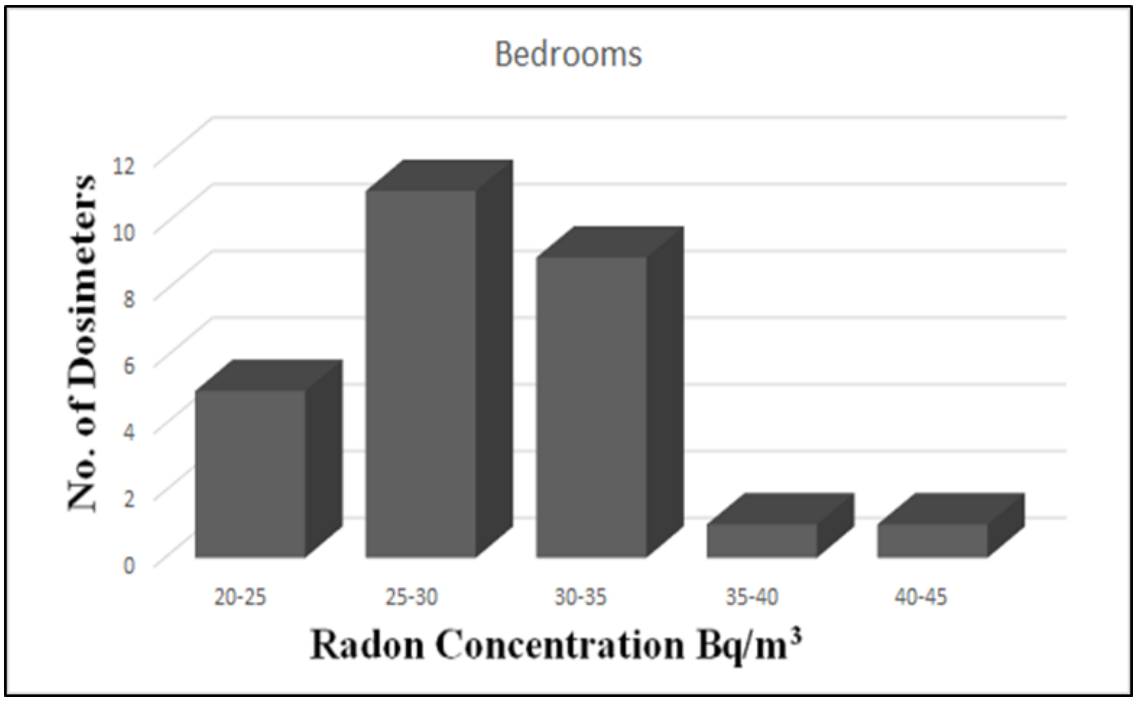

Figure 5. 12 Radon concentration distribution in bedrooms.

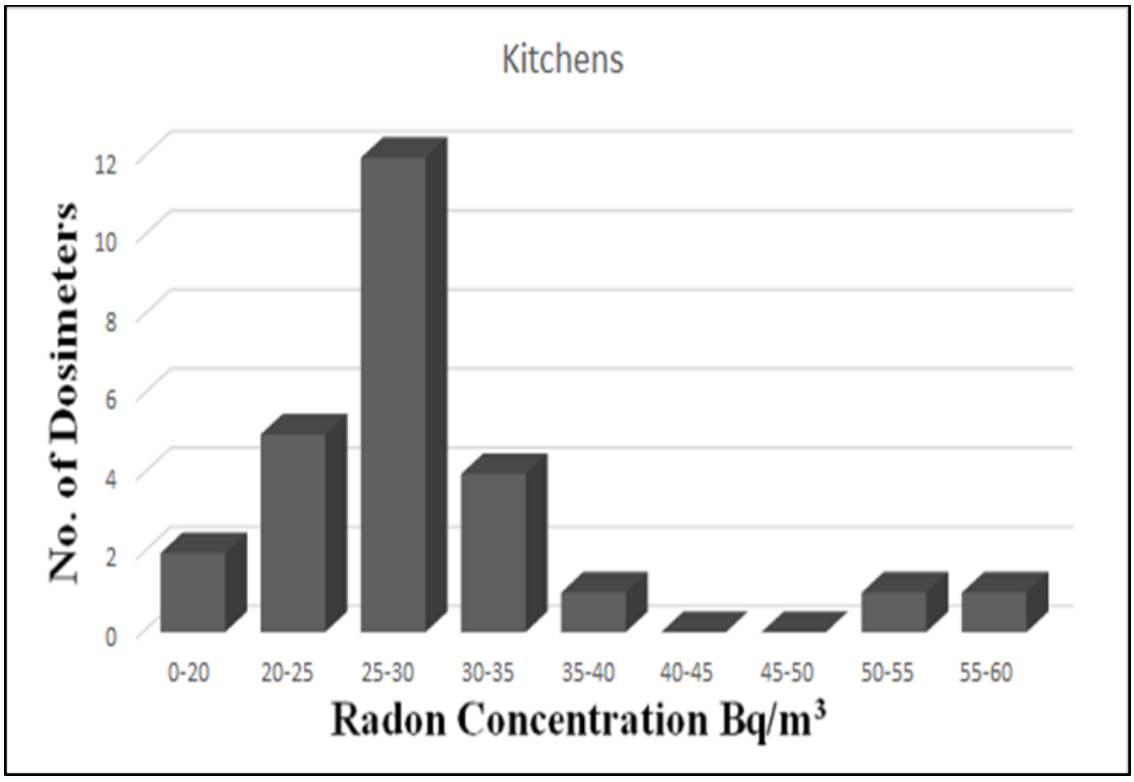

Figure 5. 13 Radon concentration distribution in kitchens

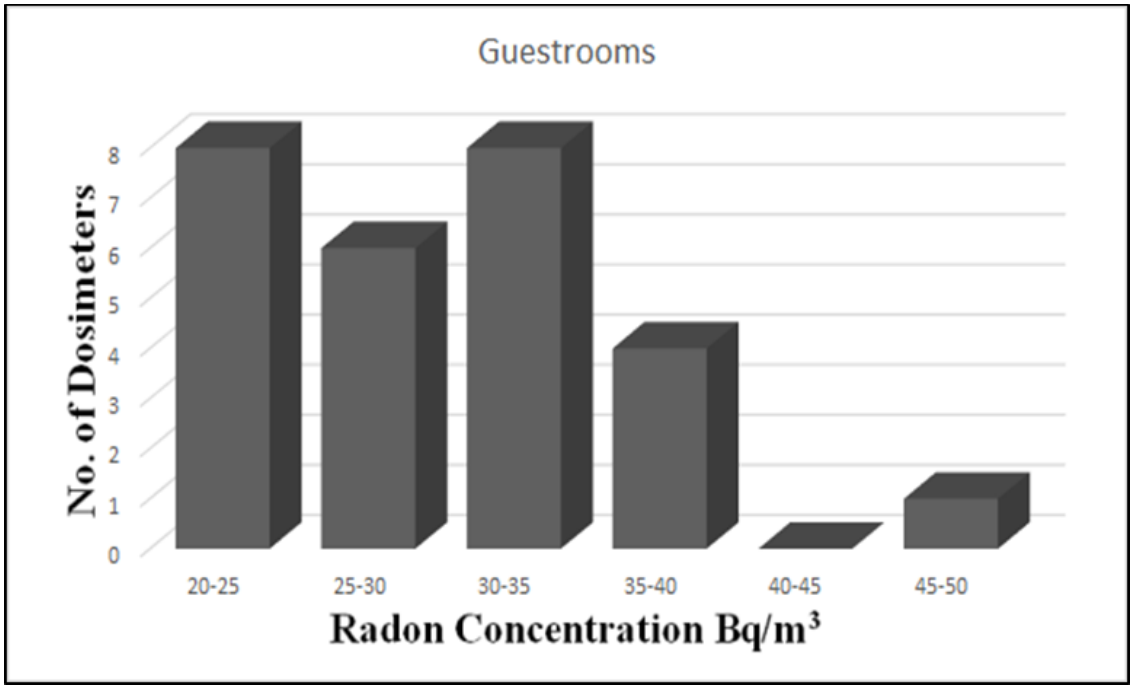

Figure 5. 14 Radon concentration distribution in Guestrooms.

5.3. A statistical t-test

In this study three main hypotheses were developed for testing: geographical area, floor level and room type. These hypotheses can be tested using statistical t-test, by finding the value of p which shows the weight of the data correlation strength. Where the hypothesis is rejected if the p value is small ($p \leq 0.05$), the hypothesis can be accepted if ($p > 0.05$).

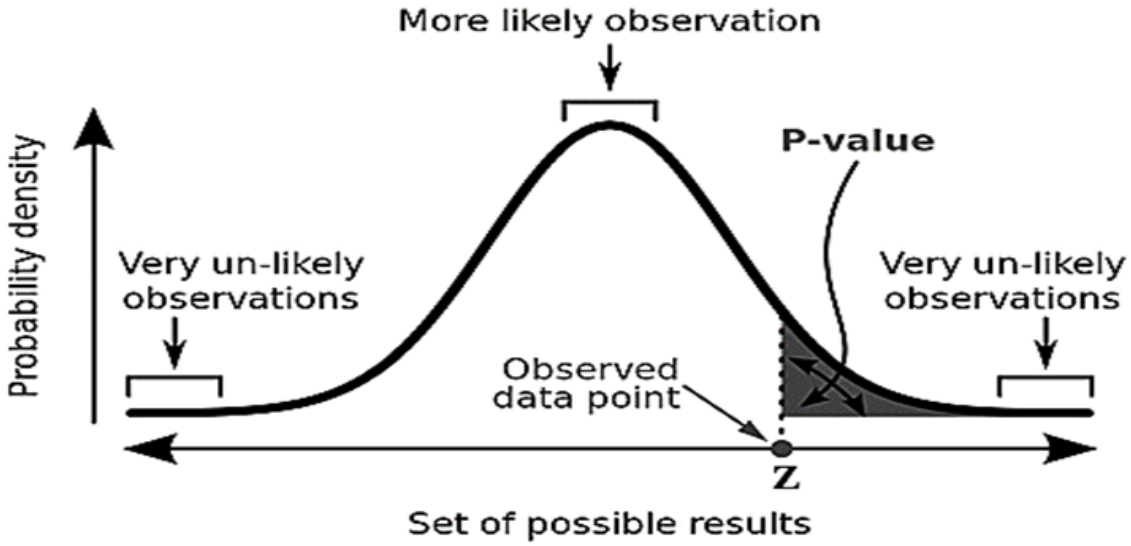

Figure 5.15 The Normal distribution

To find the value of (Z) that shown in Figure 5.15, the following formula can be used:

$$Z = \frac{Mean - \mu_0}{SD/\sqrt{N}}$$

Where: Z is test statistic and μ_0 is population mean.

Through the tables (5.11), (5.12) and (5.13), p values were calculated for pairs of regions, level of floors and rooms.

Table (5.11) P values for pairs of regions in Tammoun town.

	R1	R2	R3	R4	R5
R1		0.89	0.81	0.16	0.42
R2	0.89		0.70	0.31	0.38
R3	0.81	0.70		0.22	0.71
R4	0.16	0.31	0.22		0.05
R5	0.42	0.38	0.71	0.05	

Table (5.12) P values for pairs of level floors in Tammoun town.

	Ground floor	First floor
Ground floor		0.60
First floor	0.60	

Table (5.13) P values for pairs of type rooms in Tammoun town.

	bedroom	Guestrooms	kitchen	store
bedroom		0.79	0.89	0.30
Guestrooms	0.79		0.75	0.52
kitchen	0.89	0.75		0.57
store	0.30	0.52	0.57	

It is observed from the previous three tables that all values of p are greater than 0.05, which means that the values were not significantly different from the other, except R4 with R5 which represent the southern region with the Western Region respectively.

Chapter Six

Discussion and Conclusion

Chapter six

Discussion and Conclusion

6.1. Discussion

6.1.1. Measurements of radon in Tammoun town

The radon concentration in Tammoun town dwellings varied from 16.07 to 56.60 with average of 28.98 ± 1.22 Bq/m^3 which is below the reference level proposed by the World Health Organization (WHO) 100 Bq/m^3 (WHO 2009).

The study shows a decrease in the average of radon concentration due to several factors including:

1. 1\ The study was at the end of the summer and during the autumn season, so the wind movement is active during this period.

2. 2\ The density of buildings in the town, which is considered low.

3. 3\ Buildings built on ground containing clay soils that reduce the leakage of radon gas during it.

The annual effective dose for the town population ranged from 0.45 to 1.59 with an average of 0.74 ± 0.02 mSv / y. These numbers are below the limit allowed by the United Nations Scientific Committee on the Effects of Atomic Radiation (UNSCEAR 2008) has estimated that the global average annual dose per person from all sources of radiation in the environment is

approximately 3.0 mSv/year. In the end the risk of cancer is very low due to the low concentration of radon.

6.1.1.1 Geographical location

In all regions in town, the results of radon gas concentration were approximately equal in value. However, there may be a slight increase in the southern region because 27% of the detectors have been placed inside the homes of employees, meaning that these homes remain closed without ventilation until their residents return from work, and this increases the Radon concentration.

6.1.1.2 Floor level

The results showed that the average of radon concentration in the ground floors is higher than the floors in the first level. This is because the amount of radon leaking through the floors in contact with the earth is greater. Add to that the wind movement increases as we rise off the ground, which means exchanging air with the outside and reducing the concentration of radon inside those high floors.

6.1.1.3 Room type

The average of radon concentration between the different rooms is also small, but there is an increase in the average of radon concentration in the stores due to lack of windows and lack of ventilation. This is followed

by Guestrooms in radon concentration, whose windows and doors remain sealed and rarely used. Followed in concentration bedrooms then kitchens.

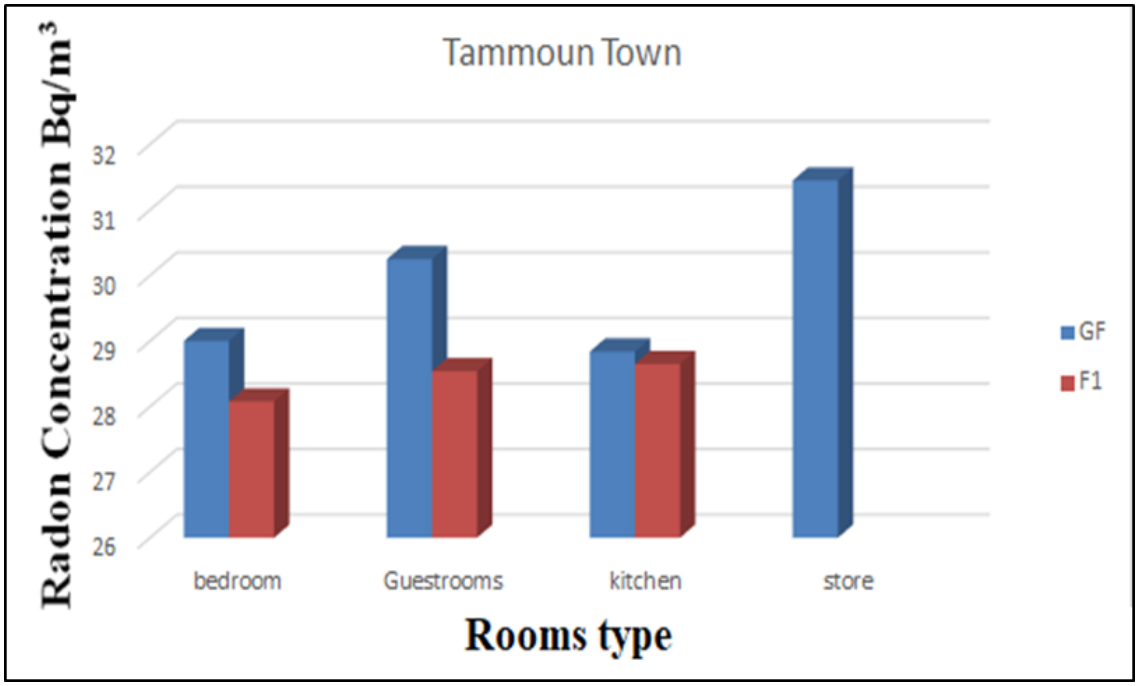

Figure 6. 1 Shows the radon concentration with room type and floor level

The figure (6.1) shows a high average of radon concentration as the floor level declines for all rooms type.

6.2. Conclusion

On the basis of this study the following conclusions were drawn:

1. This study is the first indoor radon concentration measurement that is performed in the area of Tammoun town (West Bank- Palestine).

Therefore it provides preliminary data about indoor radon levels in Tammoun town dwellings as a baseline study for a wider future national survey in Palestine.

2. The overall average indoor radon concentration in Tammoun town dwellings monitored using the SSNTDs technique was 28.98 ± 1.22 Bq/m^3. This is much lower than the USA intervention radon level of 150 Bq/m^3. Hence there are no high potential hazards in the houses investigated in this study.

3. The average annual effective dose that dwellers exposed to was found to be 0.74 ± 0.02 mSv/y which is lower than the global limit of 3.0 mSv/y. This dose corresponds to the lung cancer cases per year per million persons for dwellers in Tammoun town was worked out to be about $(1.25\pm 0.03) \times 10^{-5}$.

4. The variation of radon concentration levels with the floors confirmed the influence of soil as main source of indoor radon.

5. According to the results of the study, the radon concentration rate in the stores was the highest, then the guest rooms, due to the lack of ventilation.

6. The radon concentrations measured in this study are nearly close to the concentration level reported in previous works in Palestine such as (Jazzar & Thabayneh, 2014). But they are lower than those reported in other studies as (Abu-Samreh 2017). The higher radon concentration may be attributed to the geographical location and to the ventilation as well as the climate condition.

6.3. Recommendations

1. One of the best ways to reduce radon concentration is to increase ventilation by opening the windows, increasing their area and increasing their number. Appropriate suction fans can also be used.

2. The presence of reinforced concrete, tiles and carpets serve to reduce the leakage of radon from the ground.

3. The plastic paint can be well painted with the walls of the house, which insulates the house from the leakage of radon from the side walls.

4. There should be a distance between the soil and the ground floor when the radon concentration is high in it, to reduce its leakage to the houses.

5. The state should introduce laws prohibiting construction without taking measurements of the concentration of radon in the soil.

6. Building stones should be sampled to examine the absence of radioactive materials inside them before use.

7. Conduct new studies of radon concentration in different areas that have not been studied in order to draw a national radon contour map for Palestine.

8. Raise people's awareness of the risks of increasing the concentration of radon inside their homes.

References

*A. K.Hashim, S. S. Nayif. "**Assessment of Internal Exposure to Radon in Schools in Karbala, Iraq**." Journal of Radiation and Nuclear Applications 4, no. 1 (2019): 25-34.*

*Abu-Samreh, M., Hussain, A., Daraghmeh, M., Abu- Lebdah, A,. "**Indoor Radon-222 Concentration Levels Measurements and Exhalation Rates Calculations in Some Offices and Rooms of AAUJ during the Winter and the Spring of 2014**." Journal of the Arab American University 2, no. 1 (2016): 21-36.*

*Abu-Samreh, M., Hussain, A., Daraghmeh, M., Abu- Lebdah, A, Thabayneh, K. M.,. "**Assessment of Indoor Radon-222 Concentration Levels In Some Dwellings in Tubas City during Summer Of 2015**." Hebron University Research Journal(A) 7 (2017): 15-31.*

Aggarwal, Lalit Mohan. "**Biological Effects of Ionizing Radiation.**" SHODH PRERAK Vol. No. IV, no. 1 (January 2014): 342-348.

Al-zabadi H, Mallah K, Saffarini G,. ***"Indoor exposure assessment of radon in the elementary schools, Palestine***." *International Journal of Radiation Research 13, no*. 3 (2015): 221-228.

*Amin, Rafat M. "**Assessment of concentration and exposure doses due to radon by using CR-39 plastic track detectors in the dwellings of Saudi Arabia.**" Advances in Applied Science Research* 6, no. 7 (2015): 42-48.

Appleton, J. Donald. **"Radon in air and water**." In *Essentials of Medical Geology*, by Alloway B.J., Smedley, P. Selinus O., 239-277. Dordrecht, Netherlands, Springer, 2013.

Asere A. M, Ajayi I. R,. ***"Estimation of Indoor Radon and Its Progeny in Dwellings of Akoko Region, Ondo State, Southwestern Nigeria***." *Journal of Scientific Research & Reports* 14(3), no. 2320-0227 (2017): 1-7.

ATSDR, Agency for Toxic Substances and Disease Registry. ***Toxicological Profile for Radon.*** **Atlanta, GA: U.S.: U.S**. Department of Health and Human Services, 2012.

Burnham, J. *Radiation Protection.* **Canada: CreateSpace Independent Publishing Platform**, 2011.

Clouvas A., Takoudis G., Xanthos S., Potiriadis C., Kolovou M.,. ***"Indoor Radon Measurements in Areas of Northern Greece with Relatively High Indoor Radon Concentrations.***" *Relatively High Indoor Radon Concentrations* 136, no. 2 (Septemper 2009): 127–131.

Dabayneh. **"Indoor radon concentration measurements in Tarqumia girl schools at western Hebron region – Palestine**." *Isotope and Radiation Research* 38, no. 28 (2006): 1067-1077.

Diwan, P. K. ***Applied Physics for Engineers***. 1st edition. Wiley India, 2014.

Dwaikat N. **"Indoor Radon Concentration in four Hospitals and two Health Centers in Nablus City**." *M.Sc thesis.* An-Najah National University, 2001.

Elzain, Abd-Elmoniem Ahmed. **"Indoor Radon Concentrations in Al-Hasahisa and Rufaa Townsin the Central Part of Sudan**." *Scientific Publications of the State University of Novi Pazar* 10, no. 2 (2018): 87-98.

F. Shoqwara. ***Measurement of Radon Exhalation from Building Materials Used in Nablus District, Palestine.*** M.Sc thesis, An-Najah National University, 2012.

Gerorge, A.C. **"An overview of instrumentation for measuring environmental radon and radon progeny**." *IEEE Transactions on nuclear science* 37 (1999): 892-901.

Hanaa N. Azeez , Malik H. Kheder, Muna Y. Slewa , Sleeman Y. Sleeman. **"Radon Concentration Measurement in Ainkawa**

Region Using Solid State Nuclear Track Detector." *Iraqi Journal of Science* 59, no. 1B (Mar 2018): 482-488.

Hasan, F. "**Indoor Radon Concentration Measurements At Hebron University Campus: A Case Study**." *An-Najah J. Res* 4, no. 10 (1996): 92-107.

IAEA. "**Measurement and Calculation of radon releases from NORM residues**." *Technical Reports Series*, no. 474 (2013).

ICRP. ***Lung Cancer Risk from Radon and Progeny & Statement on Radon***. Ann. ICRP 40(1), ICRP PUBLICATION 115, 2010.

ICRP. "**Radiological protection against radon exposure**. ICRP publication 126." *Annals of the ICRP* 43, no. 3 (2014).

Jazzar M. M, Thabayneh K. M,. ***"Exposure of dwelling populations to alpha particles and its health impact in Illar region, Tulkarem - Palestine***." *International Journal of Environmental Engineering and Natural Resources* 1 (2014): 171-178.

Joseph Magill, Jean Galy. ***Radioactivity Radionuclides Radiation***. New York: Springer-Verlag Berlin Heidelberg, 2005.

Kasić A, Kasumović A, Adrović F, Hodžić M. "**Radon measurements in well and spring water of the Tuzla area,**

Bosnia and Herzegovina." *Archives of Industrial Hygiene and Toxicology* 67 (4) (2016): 332-339.

Khalef .A, Hasan .H.I, Kasim .Y.Y. **"Radon Concentration and Lung Cancer Risk in Bashika District**." *The Jordan Journal of Physics (JJP)* 9, no. 2 (2016): 81-85.

Krane, K. S. ***Introduction to Nuclear Physics.*** 3rd edition. New York: Wiley, 1988.

L'Annunziata, M. F. ***Handbook of Radioactivity Analysis***. 3rd. Amsterdam, the Netherlands: Elsevier, 2012.

Leghrouz, A., Abu-Samreh, M., Shehadeh. **"Seasonal variations of indoor radon-222 levels in dwellings in Ramallah province and east Jerusalem suburbs**." *comRadiation Protection Dosimetry* 148, no. 2 (2012): 268–273.

Miles, J. **"Methods of radon measurement and devices**." *Int Nucl Inf Syst* 36, no. 3 (2004): 146–153.

Mook WG, de Vries JJ. ***Introduction: theory, methods, review. In: Environmental isotopes in the hydrological cycle, vol 1: principles and applications***. Paris and Geneva: UNESCO and IAEA, 2001.

National Academy of Sciences. ***Comparative Dosimetry of Radon in Mines and Homes***. Washington: National Academy Press, 1991.

Nero, A.V.; Gadgil, A.J.; Nazaroff, W.W. & Revzan, K.L. ***Indoor Radon and Its Decay Products: Concentrations, Causes, and Control Strategies***. Report LBL-27798, Lawrence Berkeley, 1990.

Nidal Dwaikat, Mousa El-hasan, Masto Sueyasu, Wataru Kada, Fuminobu Sato, Ghassan Saffarini, Toshiyuki lida. **"A fast method for the determination of the efficiency coefficient of bare CR-39 detector**." *Nuclear Instruments and Methods in Physics Research Section B: Beam Interactions with Materials and Atoms* 268, no. 20 (April 2010): 3351–3355.

Obed R.I., Ademola A.K., Vascotto M., Giannini G. **"Radon measurements by nuclear track detectors in secondary schools in Oke-Ogun region, Nigeria.**" *Journal of Environmental Radioactivity* 102 (2011): 1012-1017.

Papaefthymiou H., Mavroudis A., Kritidis P., (2003). ***Indoor radon levels and influencing factors in houses of Patras, Greece.*** **Journal of Environmental Radioactivity,** 66, pp. 247–260.

Pınar köç, Neslihan Ekinci, Esra Cinan, E. Kavaz,. "**Determination of Radon Concentration by Using CR-39 PlasticTrack Detectors in Dwellings of Bingöl and Mus Provinces of Turkey**." *Asian Journal of Chemistry* 30, no. 1 (2017): 226-230.

Raymond A. Serway, Clement J. Moses, Curt A. Moyer,. ***Modern Physics*** . 3rd edition. Cengage Learning, 2004.

Smith, Blaine T. ***Pharmacology for Nurses*** . United States of America: Jones & Bartlett Learning, 2014.

UNSCEAR, United Nations Scientific Committee on the Effects of Atomic Radiation. ***Sources and effects of ionizing radiation***. Report to the General Assembly Vol. 1, New York: United Nations Publishing, 2000.

Vimercati L, Fucilli F, Cavone D, De Maria L, Birtolo F, Ferri G.M, Soleo L, Lovreglio P. **"Radon Levels in Indoor Environments of the University Hospital in Bari-Apulia Region Southern Italy**." *International Journal of Environmental Research and Public Health*, 2018: 694.

WHO, (World Health Organization). ***Handbook on Indoor Radon***. Public Health Perspective, 2009.

Annexes

Annex A: Tracks density of CR-39 detectors.

Serial No.	Dosimeter Sample No.	Room Type	Floor Level	Tracks/Field															ρ $(Tracks/cm^2)$
				Field 1	Field 2	Field 3	Field 4	Field 5	Field 6	Field 7	Field 8	Field 9	Field 10	Field 11	Field 12	Field 13	Field 14	Field 15	Average	
1	55	X	F1	3	2	2	4	4	2	3	4	3	4	3	4	4	4	3	3.27	616.35
2	44	Z	F1	4	4	5	3	2	4	3	5	5	5	3	2	3	3	4	3.67	691.82
3	22	Y	F1	2	2	3	4	2	2	3	2	2	3	2	2	3	1	3	2.40	452.83
4	26	Y	GF	1	1	2	1	2	1	2	3	2	2	3	2	1	1	2	1.73	327.04
5	58	Z	GF	3	2	4	3	3	2	2	3	3	2	2	2	4	4	2	2.73	515.72
6	36	X	GF	2	4	2	3	2	2	5	2	2	2	2	3	2	2	3	2.53	477.99
7	20	Y	GF	3	3	2	2	3	3	2	5	2	2	3	3	2	2	2	2.60	490.57
8	15	Z	GF	3	2	2	2	2	3	5	4	3	6	4	4	3	5	3	3.40	641.51
9	34	X	GF	2	2	2	3	2	4	2	2	2	2	3	3	2	2	2	2.33	440.25
10	21	Z	GF	3	4	2	2	3	3	3	2	2	3	3	2	3	3	2	2.67	503.14
11	78	X	GF	3	3	2	2	3	2	2	2	2	2	3	2	2	3	2	2.33	440.25
12	94	Y	GF																	
13	54	X	F1	3	3	4	3	2	3	4	2	2	3	2	2	3	2	2	2.67	503.14
14	91	Z	F1	2	1	3	2	2	2	2	2	2	2	2	2	2	3	3	2.13	402.52

Serial No.	Dosimeter Sample No.	Room Type	Floor Level	Tracks/Field															$\rho\ (Tracks/cm^2)$
				Field 1	Field 2	Field 3	Field 4	Field 5	Field 6	Field 7	Field 8	Field 9	Field 10	Field 11	Field 12	Field 13	Field 14	Field 15	Average	
15	8	Y	F1	2	1	4	2	2	2	4	2	2	3	3	4	4	3	2	2.67	503.14
16	73	Y	GF	3	5	3	3	4	3	5	4	3	3	3	3	3	2	2	3.27	616.35
17	97	Z	GF	2	3	4	4	4	3	2	4	4	3	4	2	3	3	5	3.33	628.93
18	13	X	GF	2	3	3	2	2	2	3	4	4	2	3	3	2	3	3	2.73	515.72
19	23	Z	F1	4	4	3	4	4	3	2	4	3	2	5	3	3	3	6	3.53	666.67
20	95	Y	F1	3	2	2	2	4	2	2	5	2	2	2	2	2	2	3	2.47	465.41
21	41	X	F1	2	2	3	2	4	2	2	7	4	3	4	4	3	6	4	3.47	654.09
22	82	Y	GF	2	2	1	2	3	1	1	1	3	2	3	3	3	1	4	2.13	402.52
23	103	W	B1																	
24	7	Z	GF	3	2	4	3	3	1	1	1	1	4	3	4	2	3	4	2.6	490.57
25	29	Y	GF	2	2	2	2	3	1	2	2	4	2	2	2	2	1	2	2.07	389.94
26	89	X	GF	5	1	2	2	2	3	2	3	2	3	1	2	4	4	3	2.6	490.57
27	74	Z	F1	3	3	2	2	3	2	2	2	2	2	2	2	2	2	2	2.2	415.09
28	31	Y	F1	3	3	2	4	2	2	6	4	3	3	2	4	3	4	4	3.27	616.35
29	75	X	F1	2	2	2	3	2	3	2	3	2	2	2	2	2	2	1	2.13	402.52
30	69	Z	F1	4	2	2	3	2	2	2	4	2	1	3	3	2	2	3	2.47	465.41

Serial No.	Dosimeter Sample No.	Room Type	Floor Level	Tracks/Field																ρ ($Tracks/cm^2$)
				Field 1	Field 2	Field 3	Field 4	Field 5	Field 6	Field 7	Field 8	Field 9	Field 10	Field 11	Field 12	Field 13	Field 14	Field 15	Average	
1	55	X	F1	3	2	2	4	4	2	3	4	3	4	3	4	4	4	3	3.27	616.35
2	44	Z	F1	4	4	5	3	2	4	3	5	5	5	3	2	3	3	4	3.67	691.82
3	22	Y	F1	2	2	3	4	2	2	3	2	2	3	2	2	3	1	3	2.40	452.83
4	26	Y	GF	1	1	2	1	2	1	2	3	2	2	3	2	1	1	2	1.73	327.04
5	58	Z	GF	3	2	4	3	3	2	2	3	3	2	2	2	4	4	2	2.73	515.72
6	36	X	GF	2	4	2	3	2	2	5	2	2	2	2	3	2	2	3	2.53	477.99
7	20	Y	GF	3	3	2	2	3	3	2	5	2	2	3	3	2	2	2	2.60	490.57
8	15	Z	GF	3	2	2	2	2	3	5	4	3	6	4	4	3	5	3	3.40	641.51
9	34	X	GF	2	2	2	3	2	4	2	2	2	2	3	3	2	2	2	2.33	440.25
10	21	Z	GF	3	4	2	2	3	3	3	2	2	3	3	2	3	3	2	2.67	503.14
11	78	X	GF	3	3	2	2	3	2	2	2	2	2	3	2	2	3	2	2.33	440.25
12	94	Y	GF																	
13	54	X	F1	3	3	4	3	2	3	4	2	2	3	2	2	3	2	2	2.67	503.14
14	91	Z	F1	2	1	3	2	2	2	2	2	2	2	2	2	2	3	3	2.13	402.52

Serial No.	Dosimeter Sample No.	Room Type	Floor Level	Tracks/Field															$\rho\ (Tracks/cm^2)$
				Field 1	Field 2	Field 3	Field 4	Field 5	Field 6	Field 7	Field 8	Field 9	Field 10	Field 11	Field 12	Field 13	Field 14	Field 15	Average	
15	8	Y	F1	2	1	4	2	2	2	4	2	2	3	3	4	4	3	2	2.67	503.14
16	73	Y	GF	3	5	3	3	4	3	5	4	3	3	3	3	3	2	2	3.27	616.35
17	97	Z	GF	2	3	4	4	4	3	2	4	4	3	4	2	3	3	5	3.33	628.93
18	13	X	GF	2	3	3	2	2	2	3	4	4	2	3	3	2	3	3	2.73	515.72
19	23	Z	F1	4	4	3	4	4	3	2	4	3	2	5	3	3	3	6	3.53	666.67
20	95	Y	F1	3	2	2	2	4	2	2	5	2	2	2	2	2	2	3	2.47	465.41
21	41	X	F1	2	2	3	2	4	2	2	7	4	3	4	4	3	6	4	3.47	654.09
22	82	Y	GF	2	2	1	2	3	1	1	1	3	2	3	3	3	1	4	2.13	402.52
23	103	W	B1																	
24	7	Z	GF	3	2	4	3	3	1	1	1	1	4	3	4	2	3	4	2.6	490.57
25	29	Y	GF	2	2	2	2	3	1	2	2	4	2	2	2	2	1	2	2.07	389.94
26	89	X	GF	5	1	2	2	2	3	2	3	2	3	1	2	4	4	3	2.6	490.57
27	74	Z	F1	3	3	2	2	3	2	2	2	2	2	2	2	2	2	2	2.2	415.09
28	31	Y	F1	3	3	2	4	2	2	6	4	3	3	2	4	3	4	4	3.27	616.35
29	75	X	F1	2	2	2	3	2	3	2	3	2	2	2	2	2	2	1	2.13	402.52
30	69	Z	F1	4	2	2	3	2	2	2	4	2	1	3	3	2	2	3	2.47	465.41

Serial No.	Dosimeter Sample No.	Room Type	Floor Level	Tracks/Field															ρ $(Tracks/cm^2)$
				Field 1	Field 2	Field 3	Field 4	Field 5	Field 6	Field 7	Field 8	Field 9	Field 10	Field 11	Field 12	Field 13	Field 14	Field 15	Average	
31	6	Y	F1	1	1	3	1	3	2	2	2	1	2	2	2	3	2	2	1.93	364.78
32	90	X	F1	2	3	2	3	2	2	2	2	2	2	4	2	3	2	2	2.33	440.25
33	96	W	GF	4	2	3	2	2	3	4	3	2	2	4	2	3	3	3	2.8	528.30
34	16	W	GF	4	3	3	3	2	3	3	2	4	4	2	3	5	2	2	3	566.04
35	57	Y	F1	4	2	5	2	6	2	2	2	3	2	6	3	3	5	2	3.27	616.35
36	40	Z	F1	2	2	2	2	3	5	3	3	3	3	6	3	3	2	3	3	566.04
37	99	X	F1	2	2	2	3	2	2	2	2	2	3	2	4	2	3	3	2.4	452.83
38	56	Z	GF	4	5	2	3	3	2	3	3	2	2	4	2	3	3	2	2.87	540.88
39	98	Y	GF	2	2	3	2	1	3	3	2	3	2	3	3	2	3	2	2.4	452.83
40	83	X	GF	2	4	2	3	5	4	2	2	2	3	2	5	3	2	3	2.93	553.46
41	71	Y	F1	9	4	7	5	7	5	2	3	4	8	3	6	4	6	8	5.4	1018.87
42	72	X	F1	2	4	4	6	2	3	2	3	3	4	2	3	3	3	4	3.2	603.77
43	87	Z	F1	4	2	3	4	3	3	3	2	3	2	2	2	4	4	3	2.93	553.46
44	100	W	GF	3	6	4	4	3	2	4	5	3	3	2	3	2	3	2	3.27	616.35
45	38	Z	F1	2	2	3	2	2	3	2	2	2	3	3	3	2	2	2	2.33	440.25
46	101	Y	F1	5	6	5	4	6	4	5	6	4	5	5	6	5	6	5	5.13	968.55

Serial No.	Dosimeter Sample No.	Room Type	Floor Level	Tracks/Field															ρ $(Tracks/cm^2)$
				Field 1	Field 2	Field 3	Field 4	Field 5	Field 6	Field 7	Field 8	Field 9	Field 10	Field 11	Field 12	Field 13	Field 14	Field 15	Average	
47	112	X	F1	2	2	2	3	2	5	3	3	3	3	2	3	2	2	2	2.6	490.57
48	1	X	F1	2	2	2	2	3	3	2	3	2	2	2	3	2	4	2	2.4	452.83
49	14	X	GF	2	3	2	2	2	2	2	2	2	3	2	3	3	2	3	2.33	440.25
50	25	Y	GF	2	3	2	4	2	2	3	2	2	2	4	2	4	4	3	2.73	515.72
51	76	Z	GF	1	2	2	3	2	2	2	2	2	2	2	2	3	2	3	2.13	402.52
52	108	Z	F1	3	3	6	2	3	4	2	2	3	3	2	2	5	2	2	2.93	553.46
53	106	W	GF	2	3	4	4	2	2	2	3	2	4	4	3	3	2	4	2.93	553.46
54	107	X	GF	3	2	3	3	3	2	4	3	2	2	3	3	2	3	3	2.73	515.72
55	105	Y	GF	3	4	2	3	2	2	1	2	2	2	2	3	4	2	3	2.47	465.41
56	28	X	F1	2	2	2	3	1	3	4	2	2	3	2	3	3	2	3	2.47	465.41
57	92	Z	F1	2	3	3	3	1	1	2	3	2	2	3	2	2	3	2	2.27	427.67
58	59	Z	GF	4	5	2	2	2	3	2	2	2	2	2	2	4	2	2	2.53	477.99
59	124	Y	GF	2	3	4	4	4	2	2	2	4	2	3	2	3	3	5	3	566.04
60	121	X	GF	3	2	5	3	3	2	3	3	3	4	2	4	2	3	2	2.93	553.46
61	104	Y	F1	2	1	2	2	2	1	1	2	2	1	1	1	1	1	3	1.53	289.31
62	43	X	F1	5	3	4	6	6	3	3	4	4	4	4	5	4	1	2	3.87	729.56

Serial No.	Dosimeter Sample No.	Room Type	Floor Level	Tracks/Field															ρ $(Tracks/cm^2)$
				Field 1	Field 2	Field 3	Field 4	Field 5	Field 6	Field 7	Field 8	Field 9	Field 10	Field 11	Field 12	Field 13	Field 14	Field 15	Average	
63	88	Z	F1	4	4	4	3	2	4	1	4	3	3	2	2	2	4	1	2.87	540.88
64	120	Y	GF	2	2	2	2	2	2	2	2	1	2	2	4	4	5	4	2.53	477.99
65	102	Z	GF	5	4	3	4	7	4	3	3	4	6	3	4	6	4	6	4.4	830.19
66	123	Z	GF	5	4	4	2	3	3	2	2	3	4	3	3	3	3	5	3.27	616.35
67	110	Z	F1	4	2	2	3	2	2	3	2	4	4	3	3	3	3	3	2.87	540.88
68	93	X	F1	3	3	3	2	5	3	5	3	4	4	4	3	3	3	2	3.33	628.93
69	122	Y	F1	4	2	4	4	4	3	3	2	3	4	4	5	2	3	4	3.4	641.51
70	12	Y	F1	2	2	4	3	5	3	2	3	2	3	2	3	2	3	3	2.8	528.30
71	39	Z	F1	4	3	4	4	3	4	4	3	3	3	3	3	5	2	5	3.53	666.67
72	81	X	F1	2	3	4	3	1	2	4	6	2	3	2	3	2	3	3	2.87	540.88
73	32	Z	GF	4	3	1	2	2	2	3	2	1	2	2	2	2	1	2	2.07	389.94
74	42	X	GF	3	5	3	2	3	4	4	3	2	3	3	5	3	3	3	3.27	616.35
75	46	Y	GF	2	3	3	2	3	4	4	2	2	2	1	2	2	3	2	2.47	465.41
76	35	X	GF	2	2	2	3	2	3	3	3	3	2	2	3	3	2	4	2.6	490.57
77	45	Y	GF	2	3	3	2	2	2	4	2	1	2	2	3	2	3	2	2.33	440.25
78	77	Z	F1	2	2	2	1	2	2	2	2	3	2	2	3	3	4	3	2.33	440.25

Serial No.	Dosimeter Sample No.	Room Type	Floor Level	Tracks/Field															ρ $(Tracks/cm^2)$
				Field 1	Field 2	Field 3	Field 4	Field 5	Field 6	Field 7	Field 8	Field 9	Field 10	Field 11	Field 12	Field 13	Field 14	Field 15	Average	
79	86	Y	F1	2	2	2	2	2	2	1	1	2	3	2	2	3	2	2	2	377.36
80	51	X	F1	3	3	2	2	5	3	4	6	3	2	3	3	3	3	3	3.2	603.77
81	59	Y	B1																	
82	11	Z	B1																	
83	19	X	B1																	
84	24	Y	GF	2	2	2	3	3	4	3	2	3	3	3	3	3	3	2	2.73	515.72
85	52	Z	GF	3	1	4	2	3	2	4	4	4	2	1	2	3	2	2	2.6	490.57
86	17	X	GF	3	2	3	3	7	2	2	2	4	4	2	2	2	2	3	2.87	540.88
87	70	Y	F1	2	2	3	2	4	4	2	2	2	2	3	5	2	2	2	2.6	490.57
88	30	Z	F1	3	3	2	2	1	2	2	2	2	3	2	2	1	2	3	2.13	402.52
89	79	X	F1	3	2	2	3	2	3	2	2	2	2	2	2	2	4	3	2.4	452.83
90	54	W	GF																	

جامعة النّجاح الوطنيّة
كلية الدراسات العليا

قياسات تركيز الرادون في المنازل في بلدة طمون، فلسطين

إعداد
محمد محمود عمر بشارات

إشراف
أ. د. غسان سفاريني

قدمت هذه الأطروحة استكمالاً لمتطلبات الحصول على درجة الماجستير في الفيزياء بكليّة الدراسات العليا في جامعة النّجاح الوطنيّة في نابلس، فلسطين.

2020م

قياسات تركيز الرادون في المنازل في بلدة طمون، فلسطين

إعداد

محمد محمود عمر بشارات

إشراف

أ. د. غسان سفاريني

الملخص

يعتبر الرادون السبب الرئيسي لسرطان الرئة بعد التدخين، حيث يتم إجراء العديد من الدراسات لتحديد تركيز الرادون داخل المنازل من أجل الحد من الأضرار التي تلحق بالناس.

الهدف من هذه الدراسة هو إيجاد مستوى تركيز الرادون في منازل بلدة طمون باستخدام تقنية قياس غاز الرادون السلبي مع كواشف مسار ألفا CR-39.

خلال فترة زمنية مقدارها ثلاثة أشهر، تم توزيع الكواشف على غرف مختلفة تقع في عدة مناطق في مستويات مختلفة من الطوابق. وبعد انتهاء الفترة تم جمع الكواشف ومعالجتها كيمائياً بمحلول (NaOH) عند تركيز 6.25 N على درجة حرارة 75 درجة مئوية لمدة 6 ساعات.

يتراوح تركيز الرادون في مساكن بلدة طمون من 16.07 إلى 56.60 بمتوسط 28.98 ± 1.22 بيكريل/م^3. بالنسبة للجرعة الفعالة السنوية لسكان البلدة تراوحت بين 0.45 إلى 1.59 بمتوسط 0.74 ± 0.02 سيفرت/سنة. واحتمال حالات الإصابة بسرطان الرئة سنويًا لكل مليون شخص من سكان البلدة [$(1.25 \pm 0.03)\times10^{-5}$].

متوسط تركيزات الرادون في الطابق الأرضي والأول على التوالي: 29.53 ± 0.92 بيكريل/م^3 و 28.76 ± 1.16 بيكريل/م^3، في حين أن متوسط تركيز الرادون لغرف النوم وغرفة الجلوس والمطبخ والمخزن كانت: 29.04 ± 0.86 بيكريل/م^3، 29.43 ± 1.16 بيكريل/م^3 ، 28.76 1.81 ±بيكريل/م^3 و 31.45 ± 1.03 بيكريل/م^3 على التوالي.

وفي النهاية فان جميع النتائج المذكورة أعلاه منخفضة ولا تؤدي إلى خطر الإشعاع على السكان.